Eastern Frequency Response Study

N.W. Miller, M. Shao, S. Pajic, and R. D'Aquila
GE Energy
Schenectady, New York

NREL Technical Monitor: Kara Clark

Eastern Frequency Response Study

N.W. Miller, M. Shao, S. Pajic, and R. D'Aquila
GE Energy
Schenectady, New York

NREL Technical Monitor: Kara Clark

NREL is a national laboratory of the U.S. Department of Energy, Office of Energy Efficiency & Renewable Energy, operated by the Alliance for Sustainable Energy, LLC.

National Renewable Energy Laboratory
15013 Denver West Parkway
Golden, Colorado 80401
303-275-3000 • www.nrel.gov

Acknowledgments

Abbreviations and Acronyms

AGC	automatic generation control
BA	balancing authority
BL	base load
CU	conventional unit
EI	Eastern Interconnection
FR	frequency response, responsive
FRCC	Florida Reliability Coordinating Council
FRO	frequency response obligation
GR	governor response, responsive
GW	gigawatt
Hz	hertz
IFRO	interconnection frequency response obligation
LBNL	Lawrence Berkeley National Laboratory
mHz	millihertz
min	minute
MISO	Midwest ISO
MMWG	Multiregional Modeling Working Group
MVA	megavolt ampere
MW	megawatt
MWCAP	MW capability
NERC	North American Electric Reliability Corporation
NG	no governor
NPCC	Northeast Power Coordinating Council
PJM	PJM Interconnection LLC
s	second
SERC	Southeast Electric Reliability Corporation
SPP	Southwest Power Pool
UFLS	underfrequency load shedding
WECC	Western Electricity Coordinating Council
WTG	wind turbine generator

Executive Summary

Frequency response, the response of the power system to large, sudden mismatches between generation and load, has recently garnered considerable attention across all three interconnections in the United States. This study was specifically designed to investigate the frequency response of the Eastern Interconnection (EI) that results from large loss-of-generation events of the type targeted by the North American Electric Reliability Corporation (NERC) *Standard BAL-003 Frequency Response and Frequency Bias Setting* (NERC 2012a)*,* under possible future system conditions with high levels of wind generation.

The main goals of this work were to:

- Create a realistic baseline model of the EI for examining frequency response
- Illustrate overall system frequency response
- Investigate the possible impact of large amounts of wind generation
- Examine means to improve EI frequency response, with the use of active power controls on wind plants.

This study focused on the evaluation of frequency response and generation control with increasing wind penetration. As such, new wind plants replaced thermal generation at existing power plant sites. This ensures that the focus remains on frequency response rather than transmission issues. The actual installation of wind generation, as with any new generation, would require an analysis of system impact and appropriate transmission system reinforcement.

Study Overview

To accomplish these goals, GE Energy worked with FirstEnergy to acquire a dynamic database representing the EI under low load conditions. This Multiregional Modeling Working Group (MMWG) database had very little wind penetration. The original database was intended for traditional stability analysis within the PJM Interconnection system, where the first few seconds of system response to critical faults and equipment tripping are of primary concern. To evaluate overall system frequency response, simulations of up to 60 s are required. The dynamic data were reviewed, suspect models identified, and necessary changes made to achieve a flat-line response in a no-disturbance simulation, a damped response in a small disturbance simulation, and an overall stable response to a large loss-of-generation event.

The dynamic representation of the EI is known to poorly reflect the observed behavior (Eto et al. 2010). To develop the desired benchmark system performance, then, broad changes were made to models throughout the system. The Lawrence Berkeley National Laboratory report, *Power and Frequency Control as it Relates to Wind-Powered Generation* (Undrill 2010), illustrates the impact of key parameters on frequency response with a small generic system. That report's insights and GE expertise on power plant control and operation were used to improve the standard database, particularly with regard to the possible root causes of the observed frequency response of the EI. Power plant models for hundreds of plants across the interconnection were modified based on

plant size, fuel, and turbine type. These changes were based on a general understanding of plant behavior, not on any knowledge of the specific behavior of individual plants. Two major groups of changes were imposed on the dynamic data set: (1) the fraction of plants providing underfrequency governor or primary response (called Kt by Undrill [2010]) was reduced from an unrealistic 80% to a more reasonable 32%, and (2) a substantial fraction of the thermal plants providing governor response were equipped with load controls that defeat the governor action by restoring the plant power to reference, predisturbance schedules. The intent was to capture EI-wide behavior. The behavior of individual plants or balancing authority areas within the system was not inspected, nor would it be meaningful for this data set.

For this investigation, several stability cases were evaluated showing EI frequency response as it evolves toward a possible high penetration of wind. The light load power flow case was deliberately selected with the expectation that it would represent one of the more challenging conditions for the EI with respect to frequency response. At the snapshot of time represented in this case, the total EI load is 272 GW. The total generation coming from wind plants was small, less than 1 GW. Most of the simulations focused on the trip of multiple thermal plants in the region of Rockport, Indiana. This 4,455-MW event is patterned after the largest loss-of-generation event in the EI for which involuntary load shedding and other stability consequences must be avoided (NERC 2012b; Eto et al. 2010). A further test against a 1,049-MW event that occurred at light load conditions was used to verify the reasonableness of the modified base case performance.

To examine the possible impact of high levels of wind penetration on the EI, new wind generation of approximately 85 GW rating, operating at a total of 68 GW production, was added across all of the NERC regions except the Southeast Electric Reliability Corporation (SERC) and the Florida Reliability Coordinating Council (FRCC). This represents an instantaneous penetration of about 40% for those regions, and of 25% for the EI as a whole. Wind generation normally displaces thermal generation during operations. Consequently, some thermal generation that would contribute to system frequency response, both inertial and primary response, will be decommitted. Other generation will stay committed but will be dispatched to lower power schedules. An initial high wind case used a displacement of governor-responsive thermal generation that reduced the overall fraction of generation providing frequency response to about 27%. Next, a modification of the high wind case that restored the fraction of generation providing frequency response back to 32% was evaluated.

Modern wind turbines and wind plants can contribute to frequency response with governor and inertial response controls. These controls are commercially available, and vary somewhat between suppliers. Their use is not widespread in North America at this time. Simulations in which these controls were enabled were examined to test mitigation options. Specifically, underfrequency governor control on wind plants was tested by holding 5% of the available wind power (about 3,500 MW for this snapshot) in reserve. Finally, a case with one type of wind turbine inertial control was also evaluated.

Key Findings and Recommendations

The dynamic model of the EI can be adjusted to more closely capture observed behavior. The EI model improvements made in this investigation were not performed with the necessary rigor to be definitive. The results, however, are encouraging and consistent with other work (NERC 2012b,c; Undrill 2012). The evidence indicates that many generators must be operating differently than the current MMWG model. Specifically, most machines must have their governors disabled or be equipped with load reference set-point controls that defeat or diminish governor response. Detailed investigation of the performance of individual units in response to actual grid events is recommended. As wind generation penetration increases throughout the EI, unit commitment and dispatch patterns will substantially depart from historical practice. For future planning analysis, commitment and dispatch that would occur under conditions of particular concern (i.e., periods of high wind generation, relatively low load, possibly high inter-area exchanges, and poor wind and solar forecasts), will need to be properly modeled. The ongoing work of the EI MMWG is aimed at improving the system model, and is expected to create a new light load case. The lack of frequency sensitivity in load modeling for the EI should be addressed as well. Attention to network frequency correction is also needed.

The overall frequency response of the EI is adequate for the cases examined. The overall frequency response of the EI to a large system event is above the frequency response obligation as currently proposed by NERC (2012b).[1] This study was not intended to verify performance of individual regions or balancing authorities. None of the conditions examined, including cases with high levels of wind generation (up to 40% penetration in all NERC regions except FRCC and SERC), resulted in underfrequency load shedding or other stability problems. The results of this analysis are based on a single credible, but challenging, system condition. It is conceivable that with a higher fidelity model or under other extreme conditions not tested in this investigation, the system could perform unsatisfactorily. Also, the study simulations assume that sufficient secondary reserves (regulation and load following) are available to handle the variability of wind generation. If secondary reserves are exhausted because of the uncertainty and variability associated with wind generation, primary frequency response capability might be drawn down before a big event occurs. This work did not attempt to quantify the specific causes or likelihood that such depleted primary reserve conditions might occur.

The fraction of generation providing governor control must be maintained above a minimum level. This study showed that the fraction of generation participating in governor control, Kt, is a primary metric for expected performance. Broadly, maintaining a minimum Kt on the order of 30% appears necessary, and is consistent with other findings. Although Kt is a good metric, details of specific operating conditions, including the relative count of generators providing governor response, the amount of headroom on those units, the frequency and voltage sensitivity of loads, and contributions from other

---

[1] According to the NERC website: "Status: A recirculation ballot for BAL-003-1 closed on December 21, 2012 with a quorum of 86.19% and 76.53% approval. The standard will be presented to the NERC Board of Trustees for adoption at its February meeting." Accessed March 5, 2013: http://www.nerc.com/filez/standards/Frequency_Response.html.

resources all play a role in determining overall frequency response. Policies and practice—like the NERC frequency response obligation—that aim to maintain minimum levels of primary response at a system level should be effective, regardless of the level of wind generation. Speed of primary response is important. Resources that provide significant incremental power before the frequency nadir are more valuable in avoiding load shedding.

Governor withdrawal on thermal plants causes a degradation in frequency response. Governor withdrawal occurs when a deliberate load control acts to nullify a plant's governor response. In this study, it caused a roughly 44% degradation in frequency response for the case with about 30% of the generation participating in governor control. About two-thirds of the responsive plants were affected, which is similar to levels found in NERC work. Measures to correct this behavior should be investigated. Any future inducements for resources (including wind power) to provide governor response should avoid aggravating this problem.

Governor response from wind plants can provide significant primary frequency response. The systemic benefit of these responses can be several times greater, per megawatt, than was observed for governor response in the synchronous fleet. Curtailment of available wind generation to provide this service would represent a substantial opportunity cost to wind plant owners. Governor controls for wind plants are commercially available and are mandated in some systems (EirGrid 2011; Alberta Electric System Operator 2010; Miller et al. 2009), but at present they are not used on wind plants in the Eastern Interconnection. The study results are based on dynamic performance available from GE type 3 (and type 4) wind turbines. Dynamic performance for wind plants using other turbines will vary depending on the manufacturer's design of these control functions.

Inertial controls on wind plants can improve the frequency nadir. Reduction in system inertia resulting from higher penetrations of renewable generation, per se, may not have a significant impact on frequency response when compared with governor action. Fast transient frequency support via controlled inertial response from wind turbines, however, was shown to significantly improve the frequency nadir.

Damping of inter-area oscillations in the EI tended to improve with wind penetration. However, further analysis is necessary to determine whether this is due to the increasing wind penetration, the associated decommitment of thermal generation, or modeling inaccuracies. Such analytical efforts can be performed in conjunction with improvements to the EI model fidelity.

Frequency response of the EI for this challenging condition with high levels of wind generation met current standards of performance. Operational options using both synchronous generation and wind plant controls can beneficially affect system performance. Changes to operational procedures, markets, and interconnection requirements could be needed to avoid frequency response problems in the future.

Contents

List of Figures

List of Tables

1 Introduction

The reliable operation of a power system depends on maintaining frequency within predetermined limits around the nominal operating frequency of 60 Hz. The frequency of an interconnection is primarily controlled by adjusting the output of generators to maintain the balance between generation and load. Other resources, including loads and energy storage devices that are under frequency control, can contribute, but today these other resources play a minor role. Failure to maintain frequency within these limits can disrupt the operation of customer equipment, initiate disconnection of power plant equipment, and possibly lead to widespread blackouts. The frequency control of a power system, then, is an essential aspect of system reliability. There is evidence that the frequency response (FR) of the Eastern Interconnection (EI) has been declining for about 2 decades (North American Electric Reliability Corporation [NERC] 2012c; Eto et al. 2010). This has raised concerns in the industry, which include the possibility that adding substantial amounts of wind power might exacerbate the situation.

1.1 Background

The balancing of load and generation for frequency and flow control occurs over multiple, overlapping time frames using different resources that fall under three categories: primary, secondary, or tertiary controls.

Primary frequency control, or FR, depends on the rapid, autonomous action of resources. Generation, in particular, responds to significant changes in system frequency. Primary frequency control actions are the first line of defense against involuntary service interruptions, which can occur within a few seconds of a system disturbance.

Secondary frequency control is the fastest centralized control in the system. Secondary control actions are usually the result of automatic generation control (AGC) instructions that are issued through a balancing authority's energy management system. They start within tens of seconds and dominate system response for the first several minutes following a disturbance.

Tertiary control encompasses dispatch actions taken by the system operator to get resources in place to handle current and future contingencies. Reserve deployment and reserve restoration following a disturbance are common types of tertiary control.

Variable energy resources, particularly wind and solar generation, present challenges for reliable operation of the power system. Their generation is variable, and in most North American systems, but not all (Electric Reliability Council of Texas 2010), they do not currently contribute to frequency control.

This study builds on recent work by the Federal Energy Regulatory Commission and the Lawrence Berkeley National Laboratory (LBNL; see Eto et al. 2010), as well as by GE and the California Independent System Operator (Miller et al. 2011; GE Energy 2010) in which FR was analyzed under conditions of high penetration of variable energy resources. These studies focused on four major impacts that increased renewable generation could have on primary frequency control actions:

- Displacement of primary frequency control reserves—the amount of primary frequency control reserves that are online and available can be reduced as the conventional generation that supplies these reserves is displaced by the economic dispatch of variable renewable generation without primary frequency control.

- Lower system inertia—because increased renewable penetration displaces synchronous generation, lower system inertia increases the rate of change of frequency immediately following disturbances.

- Location of primary frequency control reserves—the resulting redispatch of the resources (generation and demand response) that are expected to provide primary frequency control can alter system dynamics.

- Increased need for secondary frequency control reserves—the demands placed on secondary frequency control reserves will increase because of more frequent, faster, and/or longer ramps in net system load caused by variable renewable generation (GE Energy 2010).

The LBNL study also simulated the FR of the three U.S. interconnections under future wind generation scenarios. That study found that the study team "…could not reproduce the frequency response of the Eastern Interconnection to a recent recorded event involving the sudden loss of a large amount of generation." (Eto et al. 2010, p. xvii) This study takes steps toward addressing the problems identified in the LBNL work, by exploring the FR of the EI in an effort to better understand the potential impact of high levels of wind. Conditions with instantaneous penetrations up to 40% throughout all of the EI NERC regions except the Florida Reliability Coordinating Council (FRCC) and the Southeast Electric Reliability Corporation (SERC; note that FRCC and SERC have relatively poor wind resources), are considered.

1.2 Study Objectives

The objectives of this study were as follows:

- Create a meaningful baseline model of the EI for examining FR.

- Illustrate overall system FR.

- Investigate the possible impact of large amounts of wind generation.

- Examine means for improving EI FR with the use of active power controls on wind plants.

1.3 Scope of Work and Major Tasks

The study was divided into the following tasks:

- Task 1: Study Methodology—In this task, the initial system data, wind generation build-outs, and design basis events to be studied were identified and developed. In addition, the equivalent frequency calculation and the dispatch and commitment modifications necessary to accommodate additional wind were developed.

- Task 2: New Base Case Development—In this task, the new base case was developed from an original Multiregional Modeling Working Group (MMWG) 2013 light load database and validated. This included modifying the amount of conventional generation that provides underfrequency response and adding turbine load controls that will override or limit primary frequency response. The new base case simulations were compared to the measured frequency from two actual EI events.

- Task 3: FR of High Wind Penetration Case—In Task 3, the high wind penetration case was developed and evaluated. New wind generation was added to the system, with an accompanying decommitment and redispatch of other generation in the EI. The power flows in the base case were unchanged. Dynamic models of current technology wind plants were added, and the FR of this high wind case was evaluated.

- Task 4: Potential Mitigation Measures Affecting FR Under High Wind Penetration—In this task, the impacts of various potential mitigation measures to improve system FR were examined. The mitigation measures included increased governor response (GR) from synchronous generation, governor-like response from wind generation, and inertial controls from wind generation.

2 Study Method

This section presents a number of topics that contain definitions and context for the study. Specifically, definitions of critical metrics of performance are given. The sequence of cases evaluated and the method used to add wind generation to the system are described here.

2.1 Performance Metrics

Several performance metrics and performance objectives used in this report are described in this section. These definitions refer to the points labeled in Figure 1 (NERC 2004).

System Frequency for Colstrip Power Plant Outage on April 28, 1999

Point A represents the Interconnection frequency immediately before the disturbance.

Point B represents the Interconnection frequency at the point immediately after the frequency stabilizes due to governor action but before the contingent control area takes corrective action.

Point C represents the Interconnection frequency at its maximum deviation due to the loss of rotating kinetic energy from the Interconnection.

Point D represents the Interconnection settling frequency at 60 seconds after the Point A.

Figure 1. FR definitions

2.1.1 Frequency Response

FR of the entire interconnection is calculated as found in Eto and colleagues (2010):

$$FR = \frac{\Delta P}{\Delta f}\left(\frac{MW}{0.1Hz}\right)$$

where

ΔP is the change of power by all resources *in response* to a grid disturbance,[2] and Δf is the change in frequency.

This change in power normally results mostly from primary GR of synchronous generation. It also includes contributions from loads and other resources (e.g., energy storage devices) that are under frequency control. This investigation is specifically concerned with disturbances that result in loss of generation. For this calculation, ΔP is averaged over a time period of 20 s to 52 s after the event, and Δf is the change of frequency averaged over the time period from 20 s to 52 s. This is indicative of the primary response. (More discussion of the rationale for this definition is given in NERC [2012b]; discussion of the measurement of frequency can be found in Section 2.2 of this report.)

2.1.2 Frequency Nadir

This is the lowest frequency in the event, labeled Point C in Figure 1 and in NERC (2012b).

---

[2] For a system to reach equilibrium following loss of generation, the ΔP of response must equal the amount lost, but the "response" distinction is important because it is a measure of how the resources react to the *change in frequency,* regardless of the cause.

2.1.3 Frequency Nadir Time

This is the time it takes for the response to reach its nadir.

2.1.4 Settling Frequency

For results presented throughout this report, this is defined as the average frequency between 20 s and 52 s after the event starts. This is Point B in Figure 1, but it was refined to the average value over this period in NERC (2012b). The intent of this metric is to capture the frequency after the autonomous controls (mainly governors) have acted, but before centralized control (mainly AGC) acts. In practice, these behaviors overlap, so it is difficult to assign a specific post-disturbance time to make a single measurement.

2.1.5 Frequency Response Obligation

An interconnection frequency response obligation (IFRO) is established in *Frequency Response and Frequency Bias Setting Standard: Supporting Document* (NERC 2012b). The rationale and development of the obligation is described in detail in *Frequency Response Initiative Report* (NERC 2012c). The IFRO for the EI is set in that document (NERC 2012b) and was used in this study. It is calculated as the amount of generation lost in the criteria contingency divided by the maximum change in frequency. The EI FRO is 1,002 MW/0.1 Hz (i.e., 4,500 MW/0.449 Hz) according to the November 30, 2012, version of this document, which was subsequently ratified. Broadly, the intent is that the EI should always have an FR that meets or exceeds this minimum.

This obligation is based on avoiding the first stage of underfrequency load shedding (UFLS) in the EI at 59.5 Hz (NERC 2012c, Table B).[3] It takes into account the statistical expectation that the system frequency may be as much as 26 mHz low (NERC 2012c, Table A) leading into an event, and the relative difference between the frequency nadir and the settling frequency (NERC 2012c, Table D). This last element is critical in the investigation of the EI. Unlike the other North American systems, the frequency nadir in the EI is not lower than the settling frequency. This is the so-called "Lazy-L" response, and is reflected in the CB_R metric, which is "the adjustment for the differences between Point C and Value B" (NERC 2012c). It is the ratio of the expected frequency nadir to the settling frequency. In other North American systems, CB_R is greater than 1.0, meaning that the nadir is at a lower frequency than the settling frequency. The EI settling frequency is lower on average than the initial nadir,[4] though, so CB_R is limited to 1.0. As a consequence, the FRO is proportionately smaller to the design-basis event in the EI compared to the other interconnections.

2.1.6 Balancing Authority Frequency Response Obligation

Each balancing authority (BA) within an interconnection is obligated to provide its share of the total interconnection FRO. The distribution of the obligation is based on the relative size of each BA. This is calculated as follows:

---

[3] As of this report, FRCC includes UFLS settings of 59.7 Hz.
[4] In NERC (2012c), B/C is 0.964 for 41 samples.

$$FRO_{BA} = IFRO\left(\frac{Pgen_{BA} + Pload_{BA}}{Pgen_{EI} + Pload_{EI}}\right),$$

where

FRO_{BA} is the balancing authority FRO.

$IFRO$ is the Interconnection Frequency Response Obligation.

$Pgen_{BA}$ is the annual BA generation.

$Pload_{BA}$ is the annual BA load.

$Pgen_{EI}$ is the annual interconnection generation.

$Pload_{EI}$ is the annual interconnection load.

In this work an *approximate* assignment of FRO by study area was based on the power flow condition, as summarized in Table 1. The table was created using the most recent (NERC 2012b) FRO values from NERC.[5] As noted above, the FRO is only applied at the BA level – the assignment used here is solely for the purpose of understanding and reporting the regional implications of system response. The exact values to be used in assigning FRO to balancing authorities are not published at this time.

**Table 1. Approximate FRO for the Study Areas
Based on Power Flow Load and Generation**

	Load (GW)	Generation (GW)	% of EI FRO	FRO (MW/0.1 Hz)
EI	272.4	284.1	100	1002
NPCC	41.4	44.8	15.5	155
PJM	80.8	82.9	29.4	295
SERC/FRCC	107.2	114.2	39.8	399
SPP	16.9	16.7	6.1	61
MISO	26	25.4	9.2	93

Notes: NPCC, Northeast Power Coordinating Council; PJM, PJM Interconnection LLC; SPP, Southwest Power Pool; MISO, Midwest ISO; SERC, Southeastern Electric Reliability Council; FRCC, Florida Reliability Coordinating Council

2.1.7 BA Frequency Response

This is the performance of each BA, which is expected to meet or exceed the obligation at all times. It is calculated as follows:

---

[5] The exact level of the FRO has evolved. A draft document dated February 12, 2012, included somewhat higher targets (NERC 2012d). Tables using those higher targets are included in the appendix in NERC (2012d).

$$FR_{BA} = \frac{\Delta P_{BA}}{\Delta f},$$

where

FR_{BA} is the BA frequency response.

ΔP_{BA} is the change in BA power.

The frequency change is uniform across the interconnection. In the work presented here the only power change measured and included in the calculations is that of the turbine power of the responsive generation. Load and loss impacts are not considered, beyond load modeling discussions in Sections 3.1 and 3.3.3. In this work, the change in power for each study area is used to create a FR that can be reported. As noted above, while the FRO applies only to BAs, reporting FR by study area is a mechanism to illuminate regional behavior.

2.2 Frequency Calculation

This study focuses on system-wide FR. Measuring the frequency at a single node in the grid following a disturbance can be confusing and misleading. A system equivalent frequency, f, was developed and calculated as

$$f = \frac{\sum_{i=1}^{n}(MVA_i * \omega_i)}{\sum_{i=1}^{n} MVA_i},$$

where

MVA_i is the megavolt ampere rating for machine i.

ω_i is the speed for machine i.

n is the number of synchronous machines in the system.

This is the MVA-weighted average speed of synchronous machines in the system. It filters out the local swings to give a clearer measure of the system performance of concern in this study. It can be regarded analytically as the common mode of the system. Six system equivalent frequencies, for the entire EI and five study areas (NPCC, PJM, SERC/FRCC, SPP, and MISO), were calculated in this study.

2.3 Dispatch and Commitment Characterization

2.3.1 Distinct Classes of Generation

The FR of the system is dominated by the amount and type of generation committed and how it is dispatched. Throughout this report, four distinct classes of generation are identified, in accordance with their FR behavior. According to the power flow and dynamic data, each of the generators in the study system can be characterized as one of the following types:

- GR

- Base load (BL)

- No governor (NG)

- Wind.

GR units have governor models and will provide FR. BL and NG units will not provide FR. More specifically, BL units have governors blocked from increasing mechanical power, but can respond to overfrequencies. Units with no governor models will be unresponsive regardless of the sign of the frequency deviation. GR, BL, and NG units are also considered as conventional units (CU) in this study.

2.3.2   Metrics Characterizing Dispatch and Commitment

Throughout this report, tables summarize important aspects of the initial conditions used for various cases. These tables are intended to capture the critical characteristics of the generation and load, as they relate to frequency performance. Table 2 lists the reported metrics, with a brief explanation of each.

Table 2. Key to Case Summary Metrics

GR Pgen (GW)	Power generation of units with GR
GR MWCAP (GW)	Power generation (MW) capability of units with GR
GR Headroom (GW)	Headroom of units with GR
GR MVA (1,000 MVA)	MVA of units with GR
NG and BL Pgen (GW)	Power generation of units without GR
Wind Pgen (GW)	Power generation of wind
GW Capability	MW capability of all online generation units
CU Pgen (GW) (GR + BL + NG)	Power generation of CUs
Total Pgen (GW)	System generation
Total Load (GW)	System load
Wind Pgen/Total Pgen	Ratio of wind power to system generation
Kt	The ratio between GR and other CUs

The ratio of generation that provides GR to all generation running on the system is used to quantify overall system readiness to provide FR. The LBNL report (Undrill et al. 2010) introduces this ratio as a metric, Kt; the lower the Kt, the smaller the fraction of generation that will respond. The exact definition of Kt is not standardized. For this report, it is defined as "GR MWCAP/(GR MWCAP+BL Pgen+NG Pgen+Wind Pgen)" or "GR MWCAP/GW Capability." This is the ratio of power generation capability of units with GR to the MW capability of all generation units. Power capability is defined

as *equal to the MW dispatch,* rather than the nameplate rating of nonresponsive generation because these units will not contribute beyond their initial dispatch. This is a reasonable definition, but industry discussion of a standard definition of Kt is warranted.

2.4 Evolution of Study Cases

The flow chart in Figure 2 illustrates the evolution of study cases in this report. The original power flow and stability data used for all analysis were supplied by FirstEnergy. It was based on the MMWG 2013 light load operating condition in the EI. The MMWG titles for the power flow case are:

    2011 SERIES, ERAG/MMWG BASE CASE LIBRARY
    2012 LIGHT LOAD CASE, FINAL; FOR DYN

The selection of this case was intended to be a relatively extreme case for the EI from a FR perspective. Case 2 (MMWG reduced Kt) and Case 3 (new base case) were developed to modify Case 1 (clean MMWG) into one that reasonably represents the observed EI FR. Specifically, in Case 2, many GR units that provide primary FR were converted to BL units. In Case 3, turbine load controls that will override or limit primary FR were added. As the name indicates, Case 3 (new base case) was a reasonable representation of the EI under a light load condition. A large number of conventional thermal units were replaced by wind turbine generators (WTGs) in Case 4 (high wind penetration). Case 5 (increased GR), Case 6 (GR from WTGs), and Case 7 (GR and inertial controls from WTGs) were developed to test potential mitigation methods. The power flows from the original MMWG case were unchanged in all cases. The development and system performance of these seven cases is discussed in detail in subsequent sections.
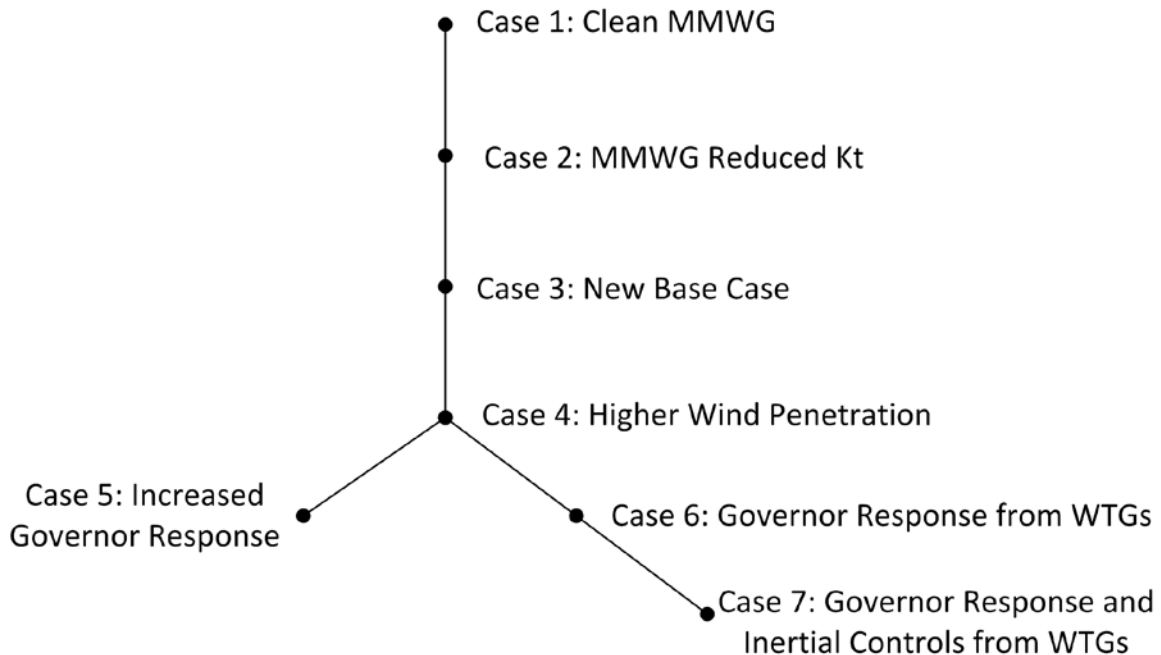
Figure 2. Evolution of study cases

2.5 Generation Trip Scenarios

Two multiplant generation tripping scenarios were evaluated in this study. These two scenarios were designed to *approximate* the megawatt loss that occurred in two real events (NERC 2012c). The first event, which occurred on August 4, 2007, at 5:44 p.m., was an approximately 4,500-MW loss of generation when the total system load in the EI was at about 480 GW (within about 5% of system peak). The second event, which occurred at 11:21 p.m. on May 13, 2012, was a 1,049-MW loss of generation. This event occurred on a Sunday when the system load was much lighter. For simulation of both generation trip scenarios, generation around Rockport, Indiana, was tripped simultaneously. No attempt was made to replicate either event in detail. The first event is used for most of the cases because it is the design basis event for the NERC FRO. The second event was added to enable a comparison of the model performance to an observed event that occurred at a load level similar to that in the model.

3 Development of a New Base Case

The development of the new base case is discussed in Sections 3.1 through 3.3. Although most of the simulations were performed for the 4,455-MW loss-of-generation scenario, simulations were also performed for the 1,060-MW loss-of-generation scenario. Comparisons of simulation results to the measured frequency from the actual events are presented in Section 3.4.

3.1 Clean MMWG Case

The original power flow and stability data used for all analysis were part of an MMWG 2013 light load case supplied by FirstEnergy.

The database provided stable response to 10-s simulation modeling faults in the FirstEnergy and PJM system. Some remote units, though, exhibited unstable behavior in the 20-s to 60-s time range of simulations.

To get a clean dynamic response in 60-s simulations, some dynamic models were modified to correct data that caused unstable response to small system disturbances. This involved minor adjustments to relatively few dynamic models. The power flow data were not changed. All simulations were done using the GE PSLF (Positive Sequence Load Flow) software.

All loads throughout the EI were modeled as static with voltage dependence. Each zonal load model had its own specific coefficients of voltage sensitivity. Models ranged from constant admittance to constant MVA. No frequency dependence was modeled. From a static load model perspective, this is a conservative modeling assumption with regard to FR (i.e., including a simple frequency-dependent term in the model would result in a better FR). In practice, static frequency sensitivity terms in load models are a simple proxy for the more complex dynamic behavior of motors and other loads. More detailed, higher fidelity load models, similar to those being implemented in the Western Electricity Coordinating Council (WECC; 2012), might result in different overall system response. This issue should be considered in the EI.

3.1.1 Case Summary

The generation information for the clean MMWG case is summarized in Table 3, using definitions presented in Table 2. The total EI generation is summarized in columns two and three of Table 3. The subsequent columns summarize the generation information for the five study areas: NPCC, PJM, SERC/FRCC, SPP, and MISO.

The first column under each study area shows the total generation and load information (listed in gigawatts) and Kt (in percentages). In the # of Units column under each area, the numbers of generators of each of the two types that are committed in the case have been counted.

The Wind Pgen (GW) row gives the instantaneous penetration of wind power. The Wind Pgen/Total Pgen row gives the instantaneous penetration as a fraction of total generation for wind power. Note that Kt is 78.9% for the EI in this case. This Kt value is significantly higher than the 30% to 40% of recent U.S. industry experience. For example, based on vetted WECC dynamic data sets that reasonably replicate observed behavior, WECC often operates with Kt in the 30%–40% range.

Table 3. Generation Summary for Clean MMWG Case

	EI	# of Units	NPCC	# of Units	PJM	# of Units	SERC/FRCC	# of Units	SPP	# of Units	MISO	# of Units
GR Pgen (GW)	202.3	1,681	34.3	398	57.3	328	74.2	594	15.0	114	21.5	247
GR MWCAP (GW)	296.0		42.8		85.9		110		26.6		30.7	
GR Headroom (GW)	93.7		8.5		28.6		35.8		11.6		9.2	
GR MVA (1000 MVA)	327.9		46.8		93.9		124.9		28.8		33.5	
NG and BL Pgen (GW)	78.3	655	10.1	330	25.2	100	40	141	0.7	35	2.3	74
Wind Pgen (GW)	0.7		0.3		0		0		0.3		0	
GW Capability	375.0		53.2		111.1		150.0		27.6		33.0	
CU Pgen (GW) (GR+BL+NG)	280.6	2,336	44.4	728	82.5	428	114.2	735	15.7	149	23.8	321
Total Pgen (GW)	281.3		44.7		82.5		114.2		16.0		23.8	
Total Load (GW)	272.1		41.4		80.8		107.2		16.6		26.0	
Wind Pgen/ Total Pgen (%)	0.2		0.7		0.0		0.0		1.9		0.0	
Kt (%)	78.9		80.5		77.3		73.3		96.4		93.0	

Notes: GR, governor responsive; BL, base load; NG, no governor; CU, conventional units; Pgen, power generation; MWCAP, power generation capability; Kt, % of CUs that are GR

3.1.2 System Response to Loss of 4,455 MW of Generation

The system response to the first generation trip scenario, a loss of 4,455 MW of generation, is shown in Figure 3 for the clean MMWG case. The blue trace (left scale) shows the FR of the EI. The frequency nadir, 59.90 Hz, occurs 2.89 s after the generation trip at 1.0 s. Within 15 s of the outage, the EI frequency has settled to a steady-state value of approximately 59.95 Hz.

The red trace (right scale) in Figure 3 shows the mechanical power output of GR units. Approximately 79% of all units have governors. The change in generation by GR units represents the vast majority of system response and is nearly equal to the 4,455 MW of lost generation. As expected, this simulation of the EI closely resembles the simple illustrative simulations in the LBNL report (Undrill 2010, Figure 4) for which all generation units had governors.

Figure 4 shows the FR for the five study areas. An inter-area oscillation mode primarily between east and west was observed. FRCC/SERC (green) and NPCC (blue) swings are approximately out of phase with SPP (pink) and MISO (black). In terms of oscillation magnitude, MISO has the most severe oscillation and PJM has the least severe oscillation. This inter-area oscillation mode settled out by the end of the simulation.
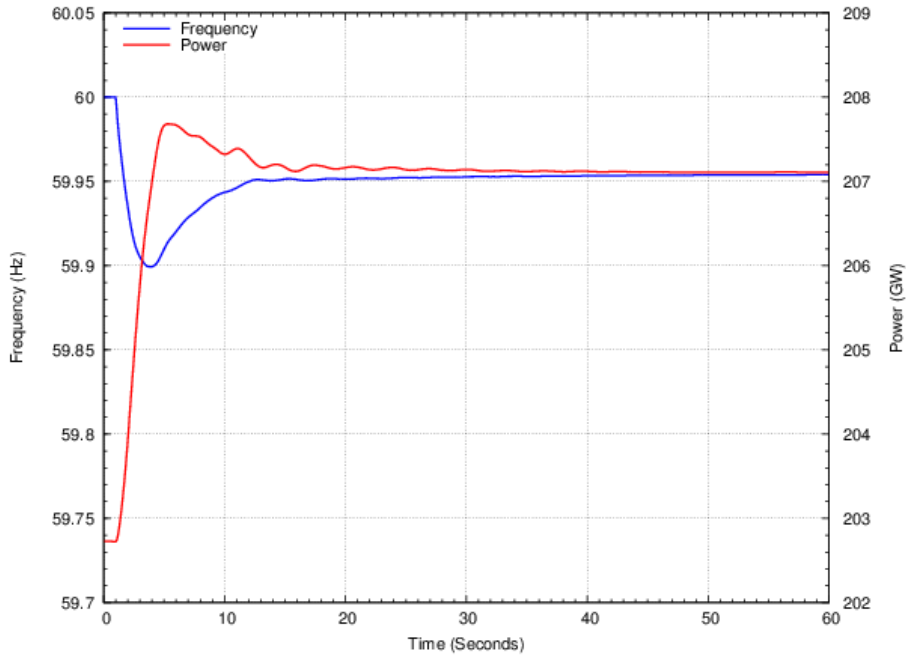
Figure 3. FR and GR to loss of 4,455 MW of generation – clean MMWG case
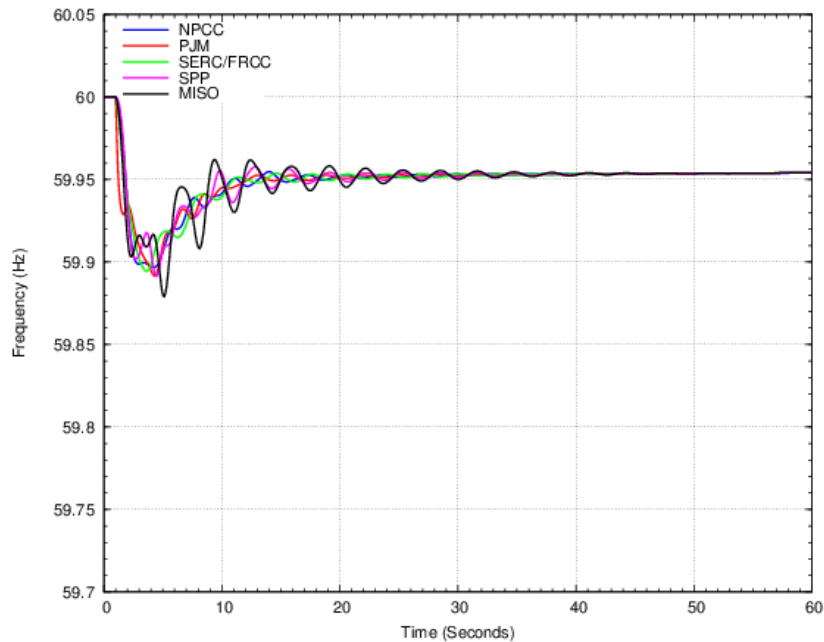
Figure 4. Area FR to loss of 4,455 MW of generation – clean MMWG case

In Table 4, the FR is summarized in column two for the entire EI and for each area. The third column gives the FR for each study area as a fraction of FR of EI. FRO is listed in column four, and the margin to FRO, or the difference between FR and FRO, is listed in column five.

In the BAL-003 standard (NERC 2012b), the calculation of FR includes the response of generation and load to changes in frequency, as discussed in Section 2.1. In this analysis,

FR is calculated based only on the response of generation. Furthermore, the values of FRO listed under each area are based on the initial load and generation in each area with respect to the total EI. The actual FRO by BA is based on total annual generation and load energy. As a result, these are approximate values of FR and FRO applied to the study areas rather than individual BAs.

Table 4. FR Summary for Clean MMWG Case

	FR (MW/0.1 Hz)	% of EI FR	FRO (MW/0.1 Hz)	Margin FR-FRO
EI	9,375	100	1,002	8,373
NPCC	1,661	17.7	155	1,506
PJM	1,785	19.0	295	1,490
SERC/FRCC	4,816	51.4	399	4,417
SPP	515	5.5	61	454
MISO	595	6.3	93	502

As noted in the background discussion, the FR of this simulation exhibits little resemblance to the observed behavior of the EI for similar events. The simulated EI FR of greater than 9,000 MW/0.1 Hz is about nine times the obligation, and many times the observed average values of about 2,200 MW/0.1 Hz (NERC 2012c).

3.2 Multiregional Modeling Working Group Reduced Kt Case

The FR of Case 1 in the previous section is at odds with observed behavior of the EI primarily because of to the governor modeling in the original data set. In the clean base case, about 80% of the units in the EI were modeled as GR. In reality, relatively few steam units provide GR to underfrequency events. Most steam units do not run throttled, but rather with valves wide open and steam supply adjusted to meet dispatch instructions (or follow the heat recovery steam generator downstream from the gas turbines in combined-cycle plants). These units would have little or no response to underfrequency events. Nuclear plants usually do not have governors enabled for underfrequency response. The bulk of the response to underfrequency events comes from hydropower, combined-cycle, and simple cycle gas units.

In this MMWG reduced Kt case, many GR units, mainly steam turbine units, were converted to BL units, in which governors are blocked from increasing mechanical power. Specifically, 501 units, with a total generation of 135 GW and a total turbine capacity of 194 GW, were converted to BL units. These units were roughly identified based on the turbine-generator model in the dynamic data and GE's overall experience with generating stations in the EI. Specific knowledge of individual units or power plants, however, was not used to modify the GR. The intent here was not to adjust the governor modeling of specific units but to adjust the response of the EI to better align with observed behavior.

3.2.1 Case Summary

Table 5 summarizes the generation information for the MMWG reduced Kt case. Compared with Table 3, the GR generation was reduced from 202.3 GW to 67.3 GW for the EI. As a result, the Kt of the EI was reduced from 78.9% to 32.4%.

Table 5. Generation Summary for MMWG Reduced Kt Case

	EI	# of Units	NPCC	# of Units	PJM	# of Units	SERC/FRCC	# of Units	SPP	# of Units	MISO	# of Units
GR Pgen (GW)	67.3	1,180	15.1	332	12.4	153	32.5	446	3.0	67	4.3	182
GR MWCAP (GW)	102.5		20.4		18.1		51.8		4.9		7.3	
GR Headroom (GW)	35.2		5.3		5.7		19.3		1.9		3.0	
GR MVA (1000 MVA)	114.7		22.1		19.6		59.8		5.2		8.1	
NG and BL Pgen (GW)	213.3	1,156	29.4	396	70.2	275	81.7	289	12.7	57	19.5	139
Wind Pgen (GW)	0.7		0.3		0		0		0.3		0	
GW Capability	316.5		50.1		88.3		133.5		17.9		26.8	
CU Pgen (GW) (GR + BL + NG)	280.6	2,336	44.5	728	82.6	428	114.2	735	15.7	124	23.8	321
Total Pgen (GW)	281.3		44.8		82.6		114.2		16.0		23.8	
Total Load (GW)	272.1		41.4		80.8		107.2		16.6		26.0	
Wind Pgen/ Total Pgen (%)	0.2		0.7		0.0		0.0		1.9		0.0	
Kt (%)	32.4		40.7		20.5		38.8		27.4		27.2	

Notes: GR, governor responsive; BL, base load; NG, no governor; CU, conventional units; Pgen, power generation; MWCAP, power generation capability; Kt, % of CUs that are GR

3.2.2 System Response to Loss of 4,455 MW of Generation

The system response to loss of 4,455 MW of generation for the MMWG reduced Kt case is shown in Figure 5. The blue trace shows the FR of the EI. The frequency nadir, 59.80 Hz, occurs 7.87 s after the event. The frequency behavior around the nadir is closer to the observed characteristics of real events, but the frequency recovery does not exhibit the withdrawal of primary FR (the Lazy-L behavior). The overall behavior is similar to the illustrative simulations of the Undrill work for a Kt of 30%. It is interesting to note that the behavior here is somewhere between the two examples in Undrill (2010), where the first example had ample headroom (Undrill 2010; Figure 5), and the second had very limited headroom (Undrill 2010, Figure 6). This suggests that the headroom in this case, of about seven times the event size, is starting to have some impact on system performance.

The red trace in Figure 5 shows the mechanical power output of GR units. Figure 6 shows the FR for the five study areas. The inter-area oscillation between east and west was still observed, but the oscillation was less damped than in the clean MMWG case.

15
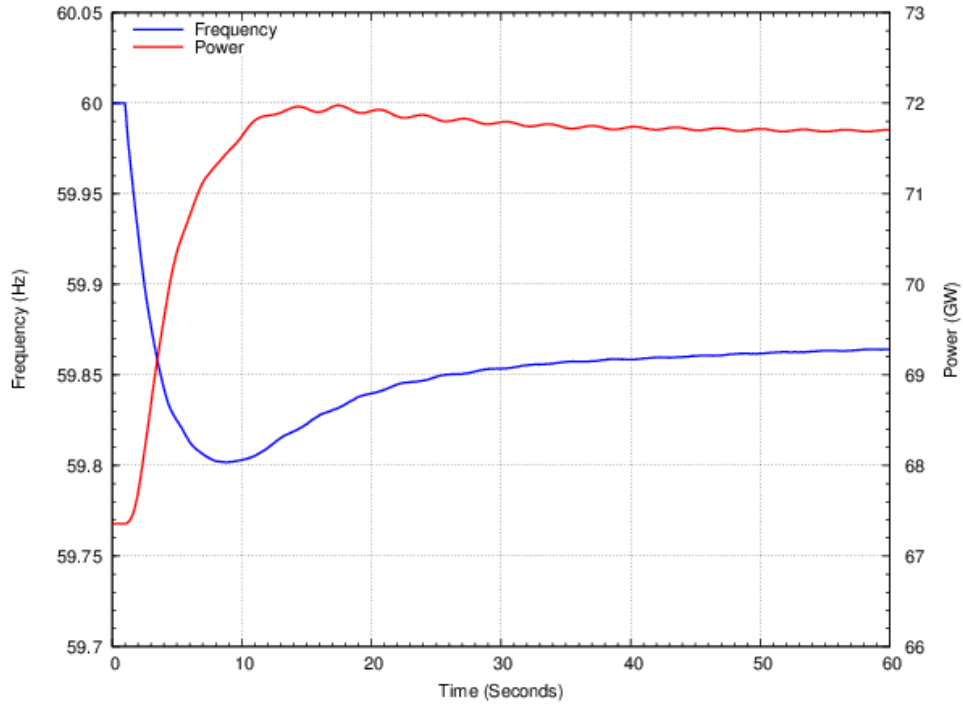
Figure 5. FR and GR to loss of 4,455 MW of generation – reduced Kt case
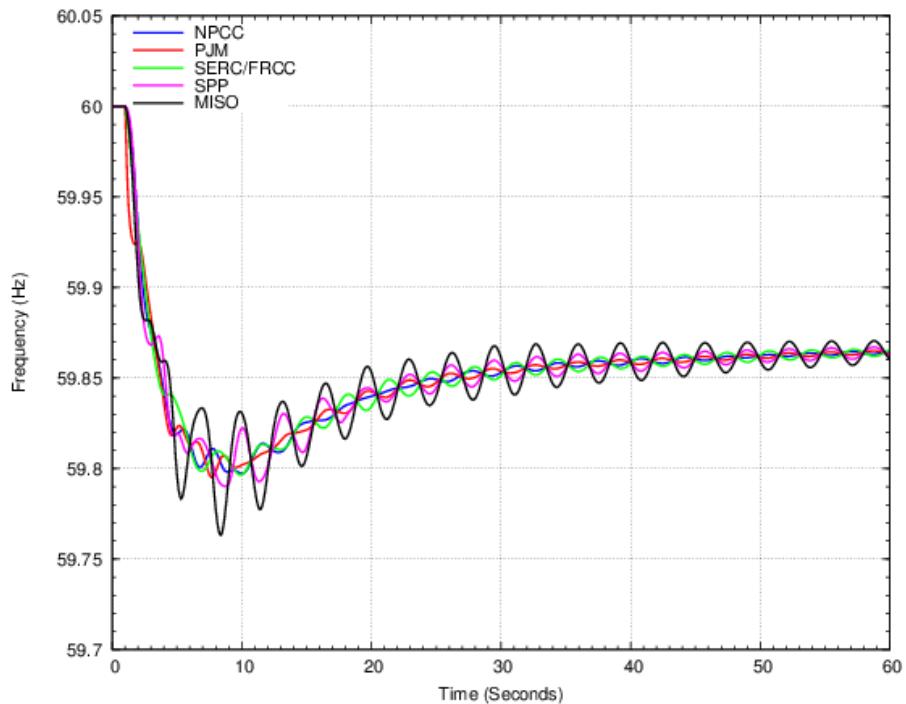
Figure 6. Study area FR to loss of 4,455 MW of generation – reduced Kt case

Table 6 lists the FR and FRO for the reduced Kt case. The FR is reduced significantly from the clean MMWG case, as expected, although it is still well above FRO for the EI and each area. As noted previously, the FR and FRO for individual study areas are given for illustration only. These values reflect the significant changes that were made to the original

16

MMWG database with respect to GR. The changes were made generically to large blocks of generation without considering specific power plants. The FR of each area is also dependent on the generation commitment and dispatch in the provided power flow case.

Table 6. FR Summary for Reduced Kt Case

	FR (MW/0.1 Hz)	% of EI FR	FRO (MW/0.1 Hz)	Margin FR-FRO
EI	3,058	100	1,002	2,056
NPCC	542	17.7	155	387
PJM	582	19.0	295	287
SERC/FRCC	1,572	51.4	399	1,173
SPP	168	5.5	61	107
MISO	194	6.3	93	101

3.3 New Base Case

The FR of the EI historically exhibits FR withdrawal (NERC 2012b). Withdrawal of primary FR results when the increase of active power output from governor action is reversed, with the total plant active power tending back to the predisturbance level. This behavior, particularly in thermal plants, results largely from the digital turbine-generator control systems, which use set point targets for generator output. These are typically outer-loop control systems that defeat the primary FR of the generators after a short time to return the unit to operating at a preset megawatt output. Undrill (2010) refers to this as "pre-selected load mode without frequency bias." Anecdotal evidence indicates that this type of control is used widely in the EI. Other physical factors affecting a sustained increase in the delivery of steam, gas, or water to turbines could also result in governor withdrawal. Phenomenon related to exhausting short-term steam supply in fossil plants could fall into this category. Unlike deliberate digital control system actions, this behavior might be more intrinsic to the plants and therefore less amenable to mitigation.

Case 2 (MMWG reduced Kt case) was modified to create the new base case, by adding turbine load controller models to the dynamic database. This model ("lcfb1" from the PSLF library), uses a closed-loop integral controller to modify the turbine power set point so that total generator output returns to the predisturbance level. This is a generic model that was adjusted to give reasonable response on the machines to which it was added. It is a proxy for the actual controls and physical behaviors specific to each plant. In this new base case, 438 GR units, with a total generation of 44.2 GW, were equipped with a turbine load controller. This represents about two-thirds of the governor-responsive generation.

3.3.1 Case Summary

Because the only difference between this new base case and the previous MMWG reduced Kt case is the added turbine load controllers, there is no change in Kt, headroom, or other metrics reported. Consequently, the generation summary for this case is the same as that for the previous case, as shown in Table 5.

3.3.2 System Response to Loss of 4,455 MW of Generation

The system response to the first loss of 4,455 MW of generation for the new base case is shown in Figure 7. The blue trace shows the FR of the EI. The frequency nadir, 59.75 Hz, occurs almost at the end of simulation at 53.464 s. The FR clearly exhibits the Lazy-L behavior expected for a large generation disturbance in the EI. The red trace in Figure 7 shows the mechanical power output of the GR units. Figure 8 shows the FR for the five study areas.
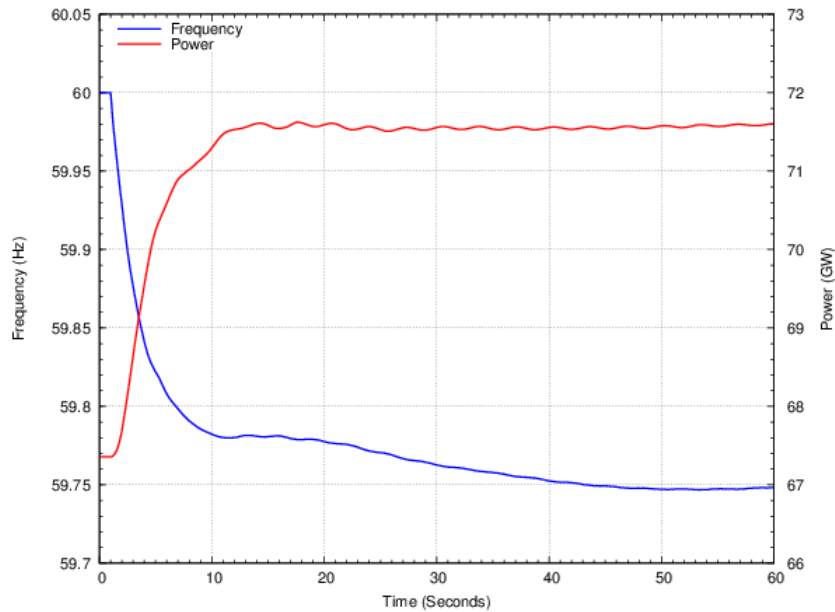

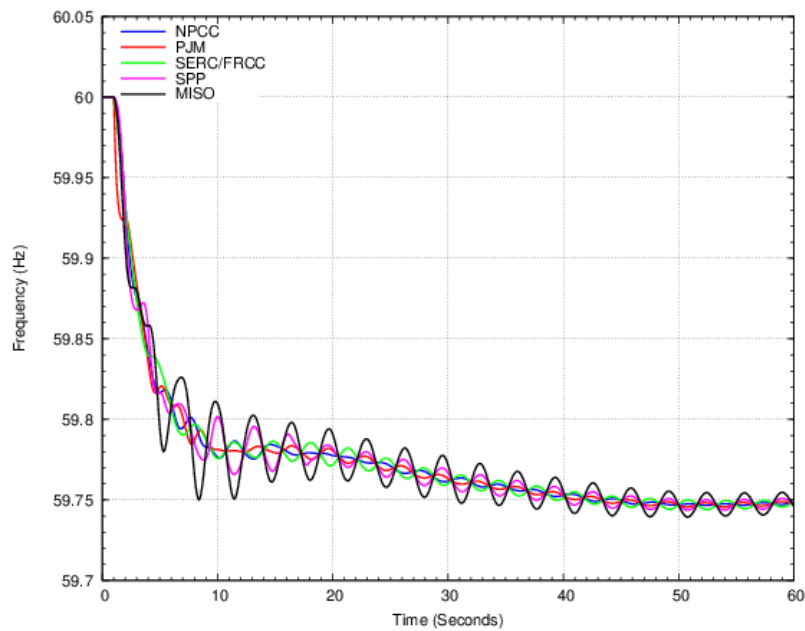**Figure 7. FR and GR to loss of 4,455 MW of generation – new base case**

Figure 8. Study area FR to loss of 4,455 MW of generation – new base case

18

Adding the effect of FR withdrawal further reduces the overall FR of the EI compared to the two previous cases. Again, the FR of individual study areas is influenced by the widespread generic changes made to the database. It does not necessarily reflect the actual response of the areas, but it does capture the overall EI response.

The linear regression of historical EI frequency response as a function of system load presented in NERC (2012c, Figure 17) indicates a mean value of about 2,100 MW/0.1 Hz at this load level. The overall average for the EI, without considering load level, is about 2,200 MW/0.1 Hz. This simulation has a smaller FR that resides in the first quartile per NERC (2012c, Figure 10).

Table 7 lists the FR and FRO for the new base case. Notice that the difference between the FR (of 1,728) in this case and the FR (of 3,058) in the previous case, a degradation of about 44%, results solely from governor withdrawal. The defeat of GR, deliberate or otherwise, has serious consequences for FR in the EI.

Table 7. Study Area FR Metrics for New Base Case – 4,455-MW Event

	FR (MW/0.1 Hz)	% of EI FR	FRO (MW/0.1 Hz)	Margin FR-FRO
EI	1,728	100	1,002	726
NPCC	368	21.3	155	213
PJM	300	17.3	295	5
SERC/FRCC	855	49.5	399	456
SPP	81	4.7	61	20
MISO	125	7.2	93	32

3.3.3 System Response to Loss of 1,060 MW of Generation

The system response to the second disturbance, loss of 1,060 MW of generation, for the MMWG reduced Kt case is shown in Figure 9. The blue trace shows the FR of the EI. The frequency nadir, 59.75 Hz, occurs almost at the end of simulation at 53.5 s. The red trace in Figure 9 shows the mechanical power output of GR units. Figure 10 shows the FR for the five study areas.
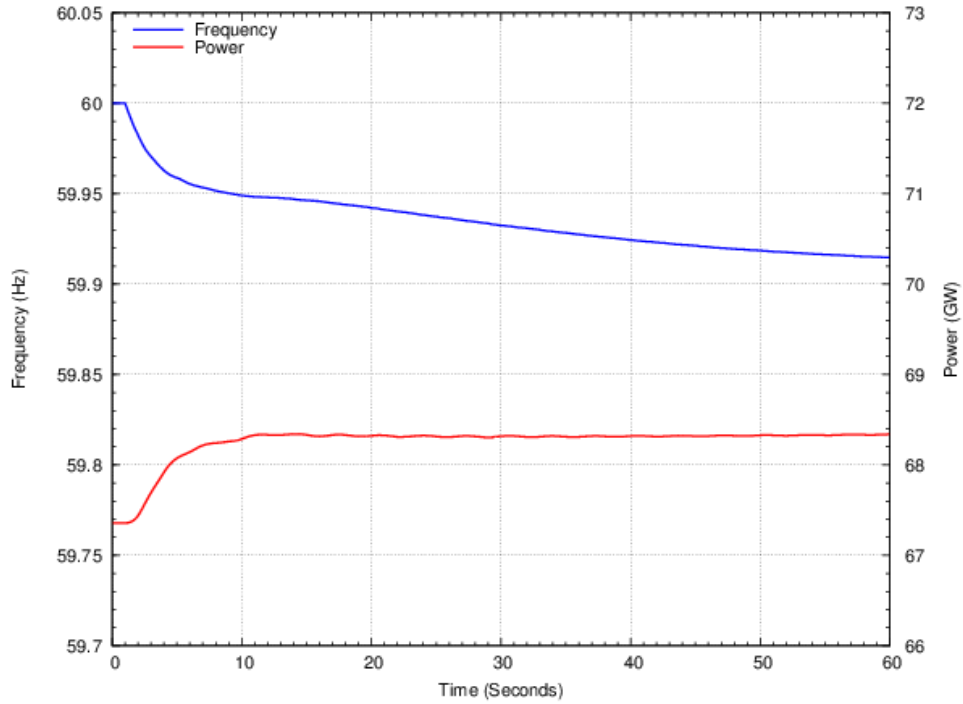
Figure 9. FR and GR to loss of 1,060 MW of generation
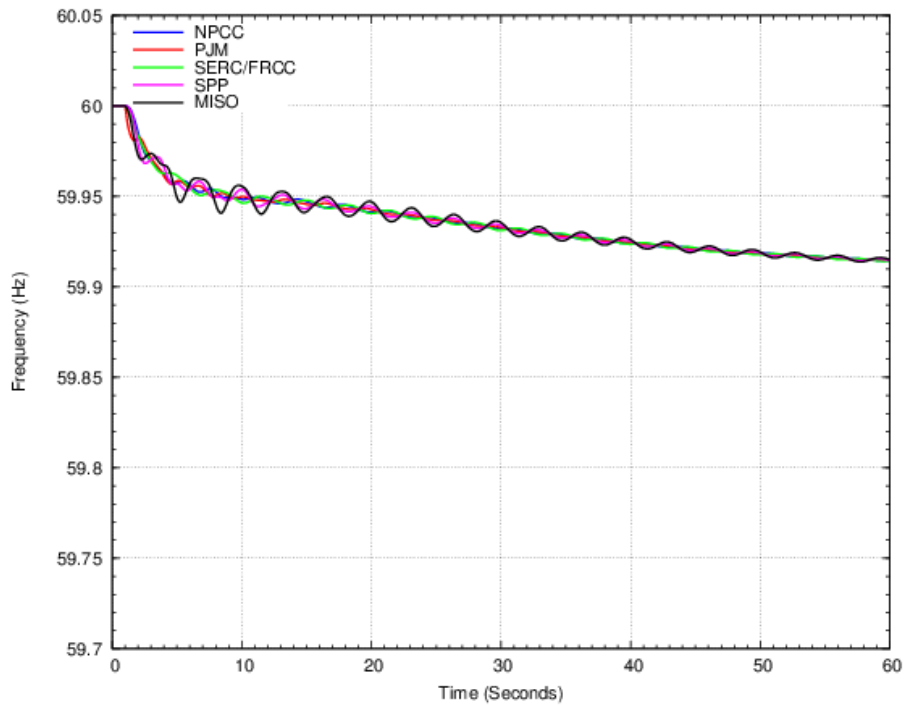
Figure 10. Study area FR to loss of 1,060 MW in generation

The FR metrics for this event with the new base case are shown in Table 8. The observed mean value of FR from NERC (2012c) is about 2,100 MW/0.1 Hz at this load level. Note that the simulated FR, 1,324 MW/0.1 Hz, for this event is substantially lower than the simulated FR, 1,728 MW/0.1 Hz, for the larger event even with the *same initial condition.*

20

Several factors might contribute to this, including control deadband effects and load voltage effects. In Miller et al. (2011), the change in system power flow patterns was observed to have a substantial impact on the bulk system voltages. Consequently, and somewhat counterintuitively, the load *voltage* sensitivity can have a bigger impact on observed system FR than the load *frequency* sensitivity. In these two cases, however, the load voltage response provided relief (load reductions) of approximately 15% of the event (e.g., ~700 MW for the 4,455-MW event) only during the first swing. Most of this beneficial response disappears after about 10 s as voltages improve, and so has little impact on the measured FR. This topic warrants further investigation because the potential impact is significant and the implied challenges for metering of FR might be substantial.

Note that the FR margin for PJM, as shown in Table 8, is negative: PJM is not meeting its obligation in the new base case. It is important to reiterate that the distribution of the FRO among the study areas is based on the conditions in the power flow (Table 1) and the original database was broadly modified to better reflect measured FR. This result, then, is purely illustrative. FRO applies to BAs only and, therefore, FRO at the study area level is not of sufficient resolution to draw conclusions. It does not indicate that BAs within PJM, or any other area, could not meet their FRO. This observation applies for all cases presented in this report.

Table 8. Study Area FR Metrics for New Base Case – 1,060-MW Event

	FR (MW/0.1 Hz)	% of EI FR	FRO (MW/0.1 Hz)[a]	Margin FR-FRO
EI	1,324	100	1,002	322
NPCC	281	21.2	155	125
PJM	217	16.4	295	–78
SERC/FRCC	649	49.0	399	250
SPP	75	5.6	61	14
MISO	102	7.7	93	9

[a] Based on NERC (2012b)

3.4 Calibration of the New Base Case

The new base case was calibrated by comparing the simulation results to the measured FR from the two events. The intent of this comparison was not to reproduce actual events, but rather to establish that the new base case reasonably captures the FR characteristics of the entire EI. As previously noted, the development of the new base case involved wholesale changes to power plant models throughout the EI. These changes were not based on specific knowledge or tests of individual plant performance.

3.4.1 Comparison to August 4, 2007, Event – Loss of 4,500 MW of Generation

On August 4, 2007, a major event included the loss of approximately 4,500 MW of generation. As noted earlier, this event is the basis for the EI FRO. Figure 11 shows the FR recorded for that event. The response exhibits the Lazy-L of primary FR withdrawal. The lowest frequency in that event, 59.868 Hz, occurred at about 1 min after the event.

Figure 12 shows the response comparison between the simulation and this August 4 event. The red trace shows the simulated FR to the simultaneous loss of 4,455 MW of generation for the new base case. The blue trace shows the measured frequency replotted from Figure 11. The overall *shape* of the frequency in the simulation is similar to that of the August 4 event.

Note that the *magnitude* of the frequency excursion in the simulation is much greater. After 30 s the depth of the frequency depression is about double (–240 mHz versus -120 mHz). This is directionally consistent with expectations. The August 4 event occurred near a peak load condition of the EI (about 480 GW of load). The simulation, however, was performed with a light load condition (272 GW of load). As a result, although the event is the same size, the system load in the simulation is roughly half that seen during the actual event. That means that roughly half as much generation would be running, and roughly half as much FR would be expected.

The qualifier "roughly" is important in this discussion. The broad-based model changes implemented to create the new base case are not based on detailed information, nor are they of sufficiently fine resolution, to duplicate the exact amplitude of the frequency excursion. It is entirely possible that the actual system FR for this event *under these light load conditions* could be higher or lower. In NERC (2012c), the authors state "there is a strong positive correlation of 0.364 between interconnection Load and Frequency Response for the 2009–2011 events. On average, when Interconnection Load changes by 1,000 MW, Frequency Response changes by 3.5 MW/0.1 Hz." The simulation is for a condition of 200 GW of lower load, so a degradation of about 700 MW/0.1 Hz would be expected based on this regression. The FR of the simulated case, at 1,728 MW/0.1 Hz, is consistent with the lower range of the regression.
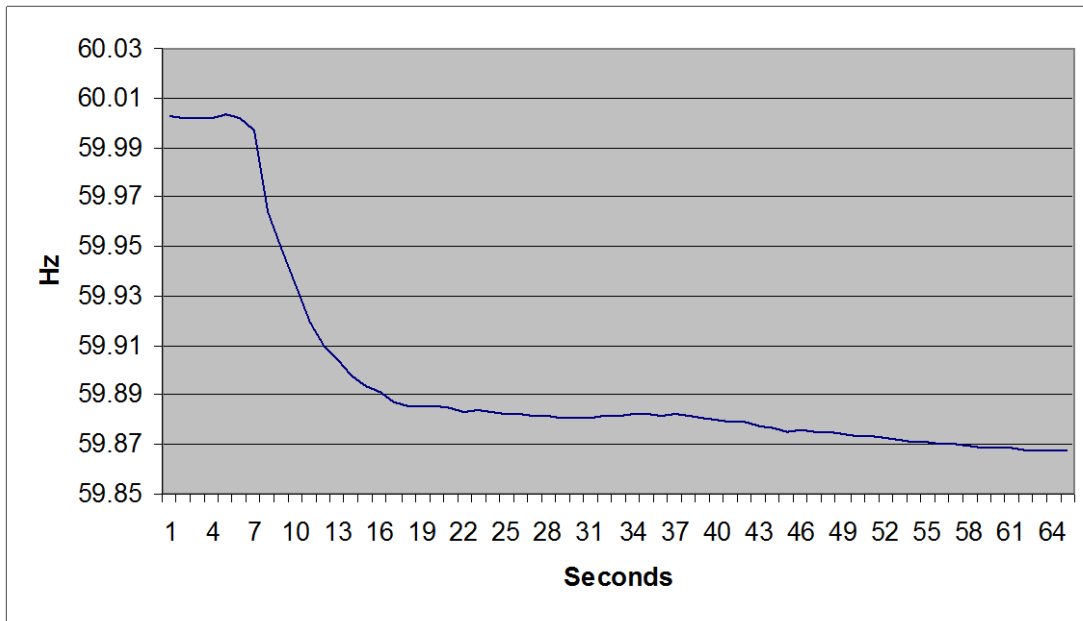

Figure 11. EI FR for loss of 4,500 MW of generation on August 4, 2007 (NERC 2012c)
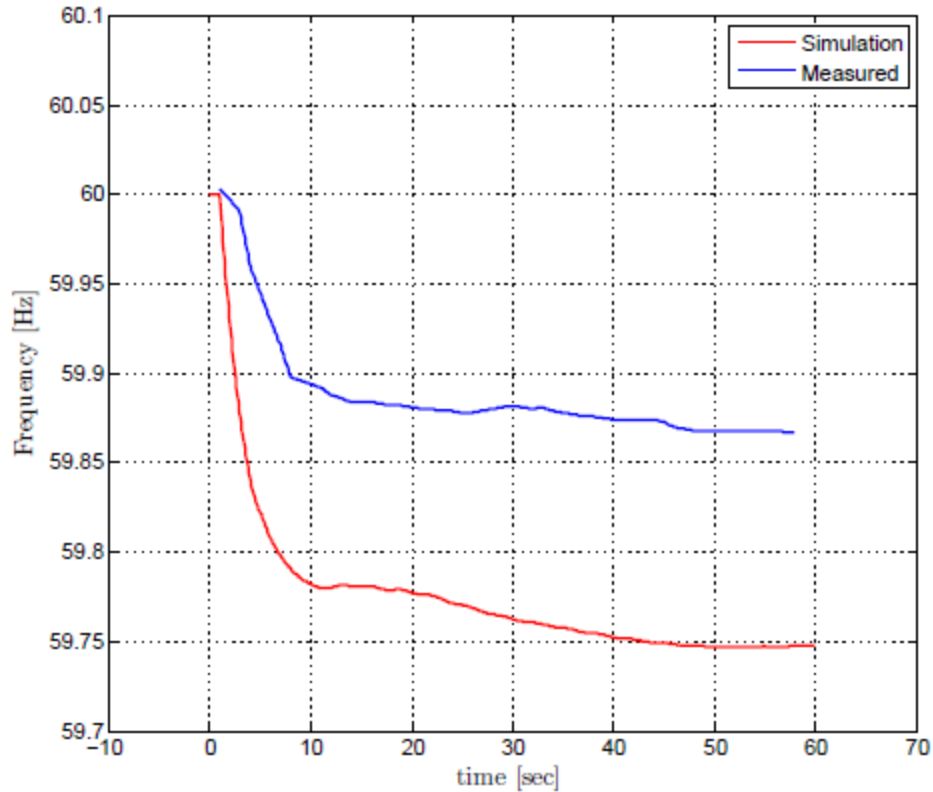
Figure 12. Response comparison between simulation results and August 4 event

3.4.2 Comparison to May 13, 2012, Event – Loss of 1,049 MW of Generation

On May 13, 2012, a less severe event occurred in which 1,049 MW of generation was lost. Figure 13 shows the frequency response for that event. Again the response exhibits the Lazy-L effect. The lowest frequency, 59.939 Hz, occurred about 1 min after the event. Note that the May 13 event represents a much lighter load condition for the EI. The system load level during this event was much closer to the load level in the New Base Case. Therefore, the match between simulation and measurement should be better.

Figure 14 shows the response comparison between the simulation and the May 13 event. The blue trace shows the simulated FR to the loss of 1,060 MW of generation for the new base case. The red trace shows the measured FR replotted from Figure 13. The blue simulation trace was shifted +0.02 Hz to account for the starting frequency of 60.02 Hz for the May 13 event. This figure shows a relatively good match between the amplitudes of the frequency excursions and in the overall shape of the FRs. The FR for the simulation (as reported in Table 8) was 1,324 MW/0.1 Hz, compared to the observed FR of 1,312 MW/0.1 Hz for the May 13 event. This shows that the new base case captures the overall FR characteristics of the EI with sufficient fidelity for meaningful examination of the impact of wind generation and of variations in control and operations strategies.
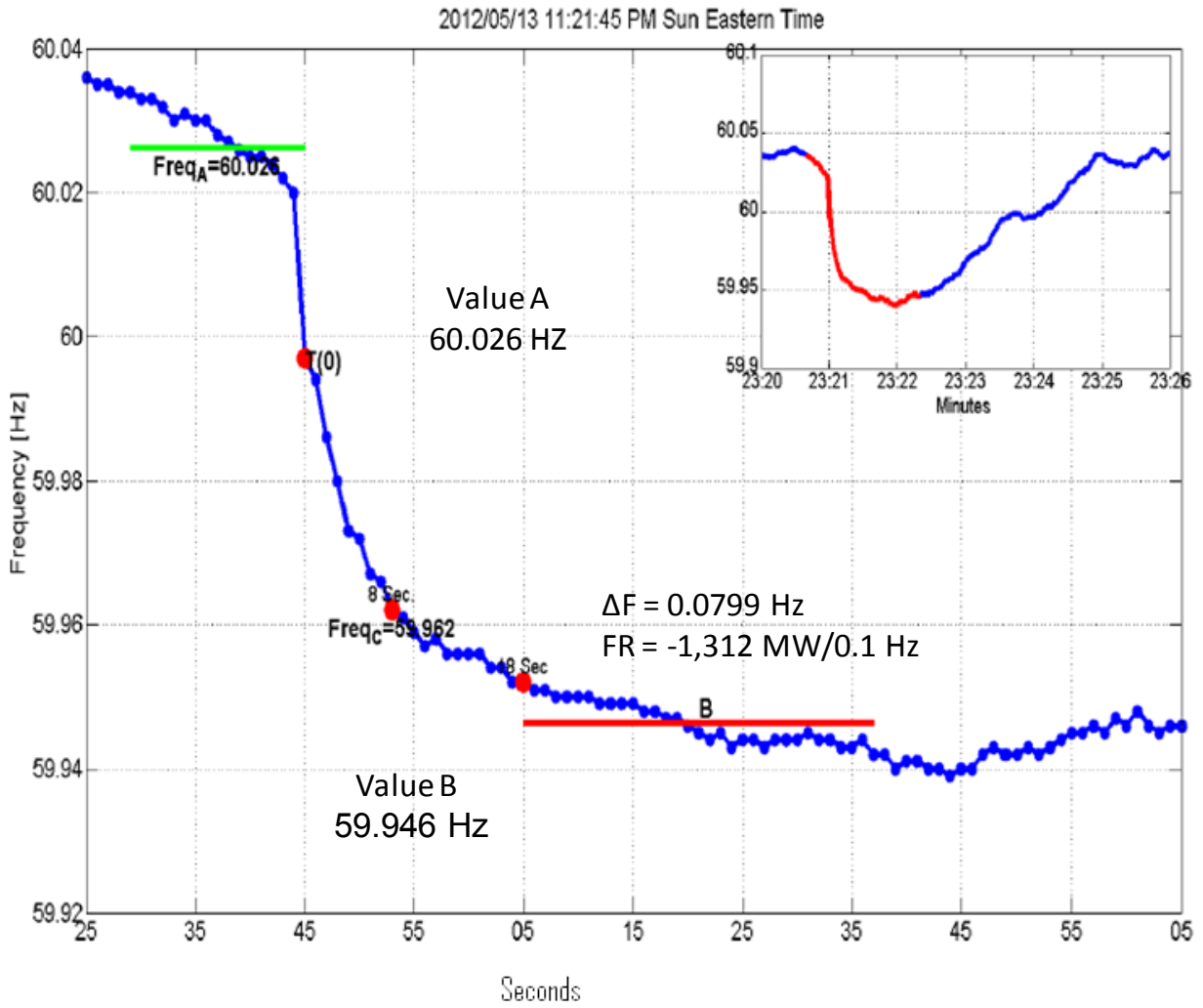
23

Figure 13. EI FR for loss of 1,049 MW of generation on May 13, 2012 (NERC 2012c)
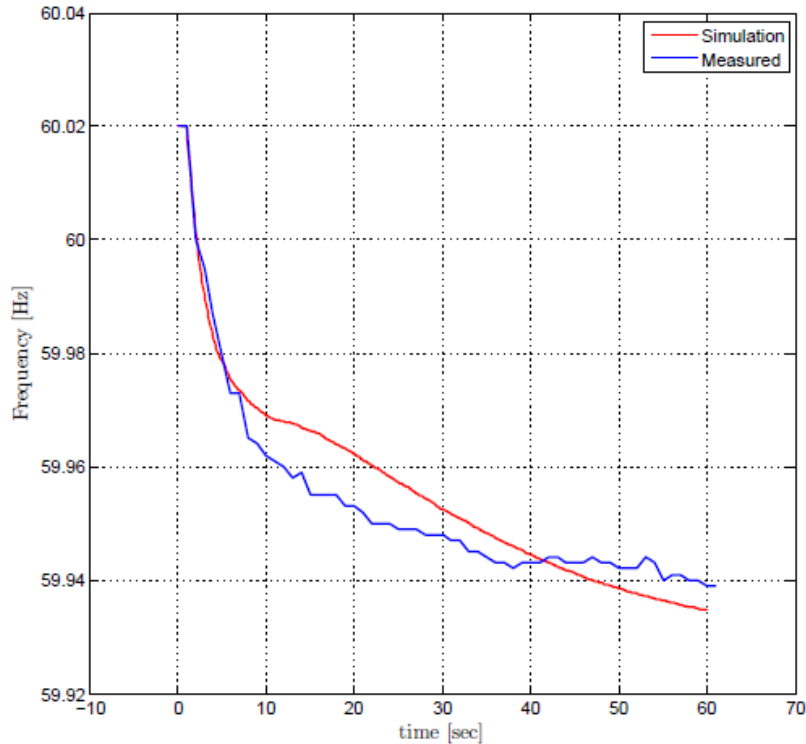
**Figure 14. Response comparison between simulation
using new base case and May 13 event**

4 Frequency Performance of High Wind Penetration Case

This section covers the development of a high wind penetration case and its FR.

4.1 High Wind Case Development

4.1.1 Forty Percent Wind Power

The level of wind generation in the previous new base case was low (about 0.2% of system load). A new case was developed to test conditions under which the entire EI hosts significant amounts of wind generation. The intent was to create some of the systemic stresses that would accompany operation with high levels of wind. No specific correlation to planned or proposed wind plants was attempted. Instead, wind was added uniformly across all portions of the EI that might reasonably host new wind generation. New wind generation was sited at existing thermal plants, and the total generation at each plant was held constant by the commitment and redispatch method described below. This approach allows the investigation to focus on frequency response and generation control without considering the additional complexities of transmission impacts.

The instantaneous wind penetration for this case is about 40% for each study area except SERC/FRCC, where little wind generation is on the horizon. With many wind plants spread across a broad geographic area, the plants are never all operating at full power at the same time. To capture a reasonably high wind condition, then, the instantaneous capacity factor of the new wind plants was randomly distributed between 0.6 and 1.0.

25

The random distribution was created using uniform probability Monte Carlo draws between these bounds.

The dynamic model of the new wind generation was based on current technology, and assumes that the wind plants meet current U.S. interconnection standards for voltage regulation and fault ride-through. The majority of wind plants being built today are either double-fed (type 3) or full converter (type 4). However, the active power dynamics are similar for both types, so all new wind plants in this study were modeled as type-3, double-fed generators with typical controls. Advanced active power controls used in later cases are based on those offered by GE. These controls, although commercially available, are not presently in widespread use.

4.1.2 Redispatch Methodology

Because adding the wind displaces other generation, the commitment and dispatch is critical to determining the FR.

Commitment and dispatch of generation in large systems is complex, and that complexity increases with substantial amounts of wind generation. It was beyond the scope of this study to fully develop specific changes to the commitment and dispatch procedures in the EI. However, the extensive economic simulations of the *Western Wind and Solar Integration Study* (GE Energy 2010) showed some broad trends relative to thermal unit displacement by wind generation. The Multi-Area Production Simulation analysis showed that for every 3 MW of additional wind production, there was on *average* a 2-MW reduction in thermal unit commitment and a 1-MW reduction in thermal unit dispatch. That average trend was used in this study, so that the incremental wind power results in two-thirds decommitment and one-third redispatch of thermal generation. In practice, such a generation displacement would depend on recent operating history, forecasts, plant availability, function, location, etc. Hydro was not redispatched because the base load flow is light-load with hydro assumed to be reduced to minimum dispatch. Further, this investigation assumes that the base case commitment and dispatch corresponds to a condition that *could* experience the relatively strong winds assumed. Detailed production simulation, including available and forecasted wind power, would be necessary to develop a case with more precise initial conditions.

Because of the high penetration of wind power, the selection of conventional thermal units (excluding hydro and nuclear) to be replaced by WTGs in each study area is constrained. A simple approach was used. Available conventional thermal units were selected in descending order of size until the 40% penetration goal was achieved. No consideration of whether displaced generation was base load or governor responsive was made in this process. It is important to emphasize that, with this method, the wind additions, thermal plant decommitments, and dispatch reductions result in exactly the same load flow condition. Only the mix of generation changes. This simplification removes the specific wind plant locations and the associated changes in transmission from consideration in this investigation. Detailed transmission studies—including consideration of reactive power, voltage, and load behavior—will be essential as the EI generation mix evolves but are not the focus of this investigation.

4.1.3 Case Summary

Table 9 shows the number of wind plants added, the total gigawatts of wind generation, the gigawatt capacity of wind generation, the gigawatts of decommitted thermal generation, and the reduction in dispatch of thermal generation that stayed online. These are shown for the EI and each study area. A total of 81.5 GW of wind turbines was added to achieve a net wind dispatch of 68.3 GW. All new wind plants used type 3 WTGs (NERC 2009).

Table 9. Wind Plants Added in EI

	EI	NPCC	PJM	SERC/ FRCC	SPP	MISO
Number of wind plants added	552	228	191	0	37	96
Power generation (GW)	68.3	18.0	33.7	0	6.5	10.1
Capacity of wind plant added (GW)	81.5	22.8	37.7	o	8.3	12.7
Approximate loading of decommitted thermal plants (GW)	46	12	22	0	4	7
Approximate dispatch reduction on committed thermal plants (GW)	23	6	11	0	2	3

Table 10 shows the generation summary for this case. Note that the wind penetration is about 40% for all study areas except SERC/FRCC. The total wind penetration for the EI is 24.2% (68.3 GW). With the displacement of thermal plants by wind plants, the total maximum power rating of GR units drops from 102.5 GW in the new base case to 85.7 GW in this high wind case. This is a fraction of the total displacement given in Table 9, and represents a drop in the fraction of generation with GR, Kt, from 32.4% in the new base case to 26.8% with the added wind generation. The headroom on GR units increased to 37.4 GW from 35.2 GW.

Table 10. Generation Summary for High Wind Penetration Case

	EI	# of Units	NPCC	# of Units	PJM	# of Units	SERC/FRCC	# of Units	SPP	# of Units	MISO	# of Units
GR Pgen (GW)	48.3	973	7.0	218	5.3	103	32.5	446	1.4	54	2.0	152
GR MWCAP (GW)	85.7		13.4		11.1		51.8		4		5.5	
GR Headroom (GW)	37.4		6.4		5.8		19.3		2.6		3.5	
GR MVA (1000 MVA)	96.3		14.2		12.1		59.8		4.2		6.2	
NG and BL Pgen (GW)	165.7	834	19.7	282	43.7	136	81.7	289	8.5	35	12.5	92
Wind Pgen (GW)	68.3		17.7		33.7		0		6.5		10.1	
GW Capability	319.7		51.1		88.5		133.5		19.0		28.1	
CU Pgen (GW) (GR + BL + NG)	214.0	1807	26.7	500	49.0	239	114.2	735	9.9	89	14.5	244
Total Pgen (GW)	282.3		44.7		82.7		114.2		16.4		24.6	
Total Load (GW)	272.1		41.4		80.8		107.2		16.6		26.0	
Wind Pgen/ Total Pgen (%)	24.2		40.3		40.7		0.0		39.6		41.1	
Kt (%)	26.8		26.2		12.5		38.8		21.1		19.6	

Notes: GR, governor responsive; BL, base load; NG, no governor; CU, conventional units; Pgen, power generation; MWCAP, power generation capability; Kt, % of CUs that are GR

4.2 Response to Loss of 4,455 MW of Generation

The system response to loss of 4,455 MW of generation for the high wind penetration case is shown by the red trace in Figure 15. As expected, the FR was worse because Kt was reduced (i.e., fewer units with underfrequency GR were committed). The frequency nadir, 59.73 Hz, occurs 10.36 s after the event. For comparison, the system response to the same loss of 4,455 MW of generation for the new base case is shown by the blue trace in Figure 15. The frequency nadir for the new base case is 59.75 Hz, occurring at 53.5 s.

Many of the units displaced in the high wind penetration case have load control resulting in governor withdrawal. Although the wind turbines are not frequency-responsive, they hold a constant level of megawatts following the disturbance. With a lower Kt, the nadir is deeper and occurs sooner, but because fewer units are on load control, the final frequency at 60 s is 15 mHz lower. Different assumptions about displaced generation will change the response with high wind penetration.

Figure 16 shows the GR to the loss of 4,455 MW of generation for both the new base case and the high wind penetration case. Figure 17 shows the wind power generation. This plot shows that 68.3 GW of wind power is constant, as expected, because the wind plants in this case have no FR controls. Figure 18 shows the FR for the five study areas.

Note that the damping of the inter-area oscillations has inadvertently improved over the new base case (see Figure 8). This may be a result of the high damping contribution that naturally accompanies type 3 wind generation (Sanchez-Gasca et al. 2004), but further investigation into system damping would be required to establish the fidelity of this aspect of the simulation and the causes of the improved damping.
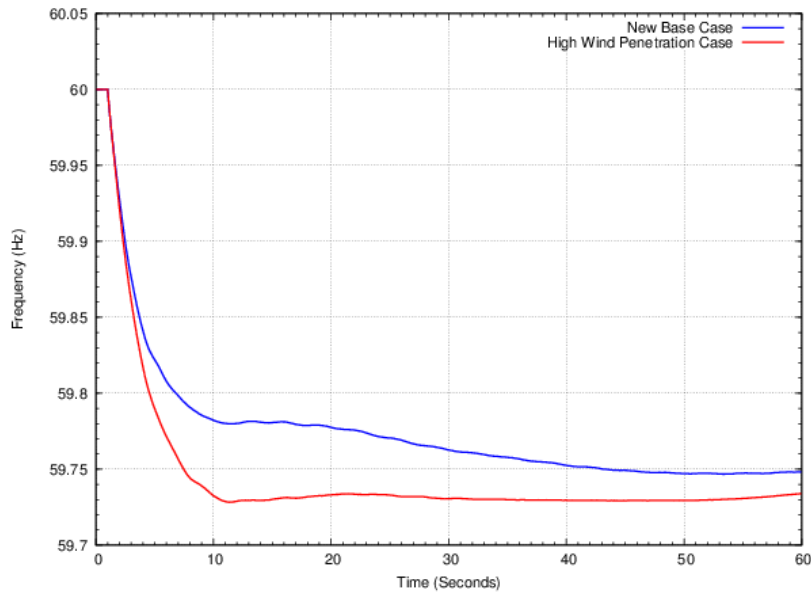

Figure 15. FR comparison – new base case (blue) versus high wind penetration case (red)
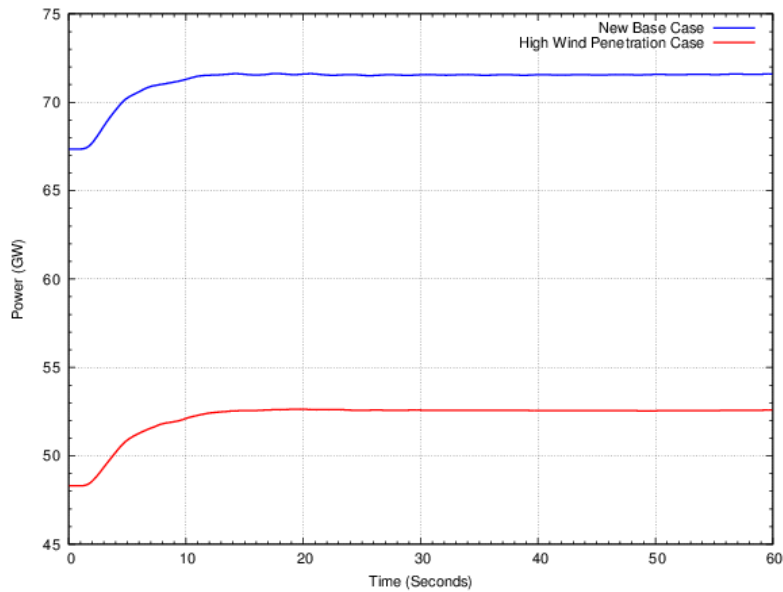

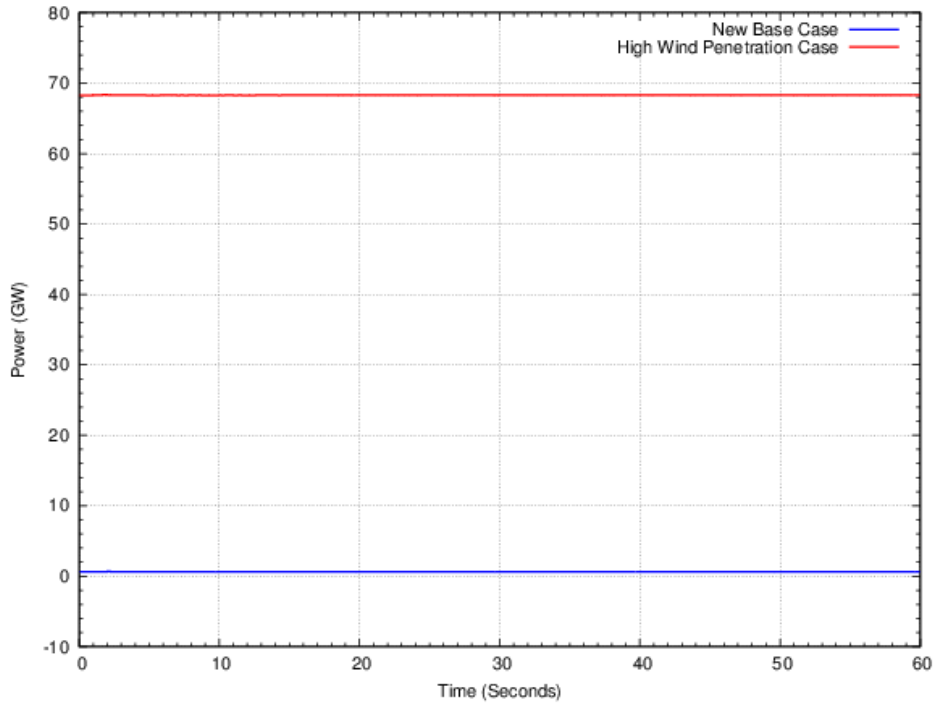**Figure 16. GR comparison – new base case (blue) versus high wind penetration case (red)**

Figure 17. Wind power – new base case (blue) versus high wind penetration case (red)
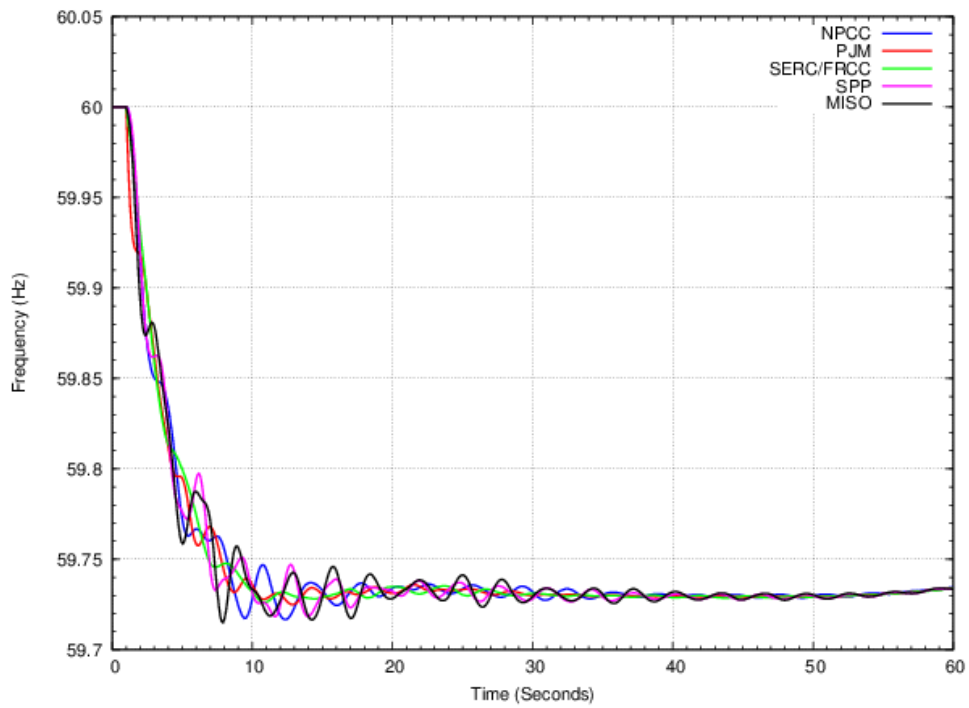

Figure 18. Study area FR for high wind penetration case

The FR of the EI is reduced from the new base case but still meets the IFRO with some margin, as shown in Table 11. This suggests that ignoring FR in the redispatch and decommitment process, although likely to degrade system performance, does not necessarily create problems or violations of the FRO.

Table 11. Study Area FR Metrics for High Wind Penetration Case

	FR (MW/0.1 Hz)	% of EI FR	FRO (MW/0.1 Hz)	Margin FR-FRO
EI	1,583	100	1,002	581
NPCC	380	24	155	225
PJM	160	10.1	295	−134
SERC/FRCC	856	54.1	399	458
SPP	89	5.6	61	29
MISO	97	6.1	93	4.5

5 Potential Mitigation Measures

In this section, three potential means to increase system FR are examined. All simulations were of the loss of 4,455 MW of generation.

5.1 Increased Governor Response

In this test, the number of units providing GR was increased. To accomplish this, 48 BL units in SERC/FRCC were converted to GR units. These units had a total dispatch (Pgen) of 13.6 GW and rated capability (MWCAP) of 19.1 GW. The generation summary for this modified high wind penetration case, also known as the increased GR case, is shown in Table 12. This restores the fraction of generation providing GR, Kt, of the EI to 32.3%. Note that the Kt in SERC/FRCC was increased to 51.0%. By contrast, Kt was 12.5% for PJM, unchanged from the high wind penetration case. Similarly, Kt was unchanged for NPCC, SPP, and MISO. This case, then, also offers insight into the impact of responsive generation location on overall EI frequency response.

The wind penetration for each study area and the entire EI stays the same.

Table 12. Generation Summary for High Wind Penetration with Increased GR Case

	EI	# of Units	NPCC	# of Units	PJM	# of Units	SERC/FRCC	# of Units	SPP	# of Units	MISO	# of Units
GR Pgen (GW)	61.8	1,021	7.0	218	5.3	103	46.1	494	1.4	54	2.0	152
GR MWCAP (GW)	105.0		13.4		11.1		70.9		4		5.5	
GR Headroom (GW)	43.2		6.4		5.8		24.8		2.6		3.5	
GR MVA (1,000 MVA)	118.1		14.2		12.1		81.6		4.2		6.2	
NG and BL Pgen (GW)	152.1	786	19.7	282	43.7	136	68.1	241	8.1	35	12.5	92
Wind Pgen (GW)	68.3		18		33.7		0		6.5		10.1	
GW Capability	325.4		51.1		88.5		139.0		18.6		28.1	
CU Pgen (GW) (GR + BL + NG)	213.9	1,807	26.7	500	49.0	239	114.2	735	9.5	89	14.5	244
Total Pgen (GW)	282.2		44.7		82.7		114.2		16.0		24.6	
Total Load (GW)	272.1		41.4		80.8		107.2		16.6		26.0	
Wind Pgen/ Total Pgen (%)	24.2		40.3		40.7		0.0		40.6		41.1	
Kt (%)	32.3		26.2		12.5		51.0		21.5		19.6	

Notes: GR, governor responsive; BL, base load; NG, no governor; CU, conventional units; Pgen, power generation; MWCAP, power generation capability; Kt, % of CUs that are GR

The system response to the loss of 4,455 MW of generation for this case is shown by the red trace in Figure 19. The EI FR of this increased GR case is better. Both the frequency nadir and the settling frequency are higher than in the high wind penetration case. The frequency nadir, 59.78 Hz, occurs 9.20 s after the event. For comparison, the system response to the same loss of 4,455 MW of generation for the high wind penetration case is shown by the blue trace in Figure 19. The restoration of about 14 GW of GR from thermal units improves the frequency nadir by about 50 mHz and the settling frequency by about 70 mHz.

Figure 20 shows the FR for the increased GR case and the new base case. Both cases have a similar frequency nadir in the first 15 s. This is expected because both cases have the same system Kt. With less withdrawal in the increased GR case, however, the final frequency settles higher than in the new base case. The case with high wind generation exhibits a slightly faster rate of frequency decline and hits the frequency nadir sooner. This is consistent with the reduction in system inertia when type 3 WTGs, which exhibit no inertial behavior, displace synchronous machines. The more rapid decline in frequency is not a problem in this case, but it tends to increase the need for rapid GR.

Figure 21 shows the comparison of system GR and Figure 22 shows the comparison of WTG power generation for the two different high wind cases. The FR of the study areas is shown in Figure 23 for the increased GR case.
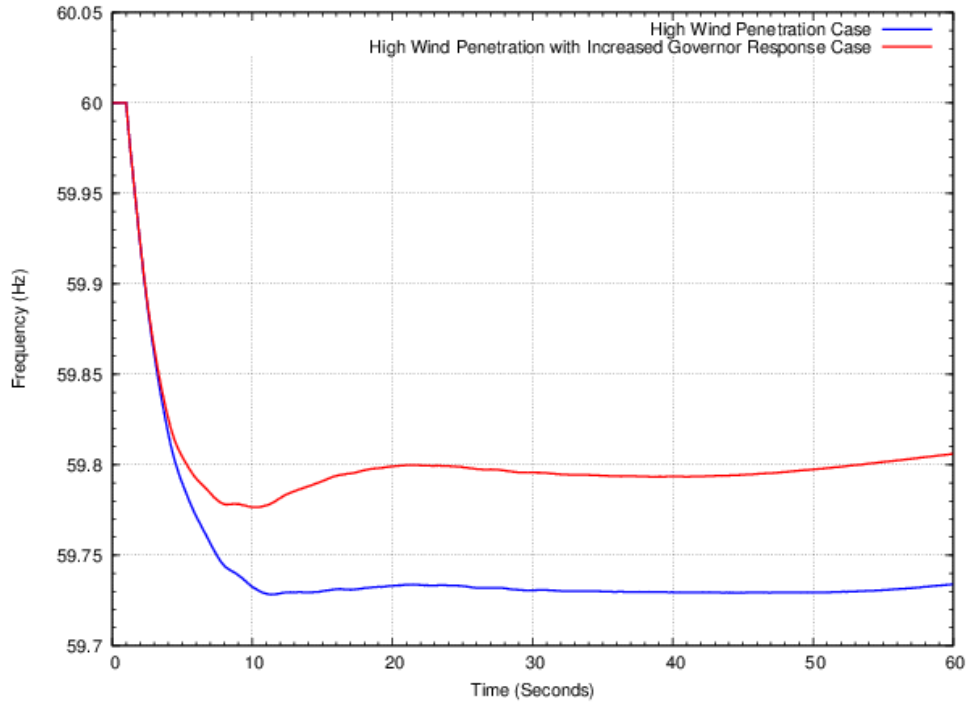
Figure 19. FR comparison – high wind penetration versus increased GR cases
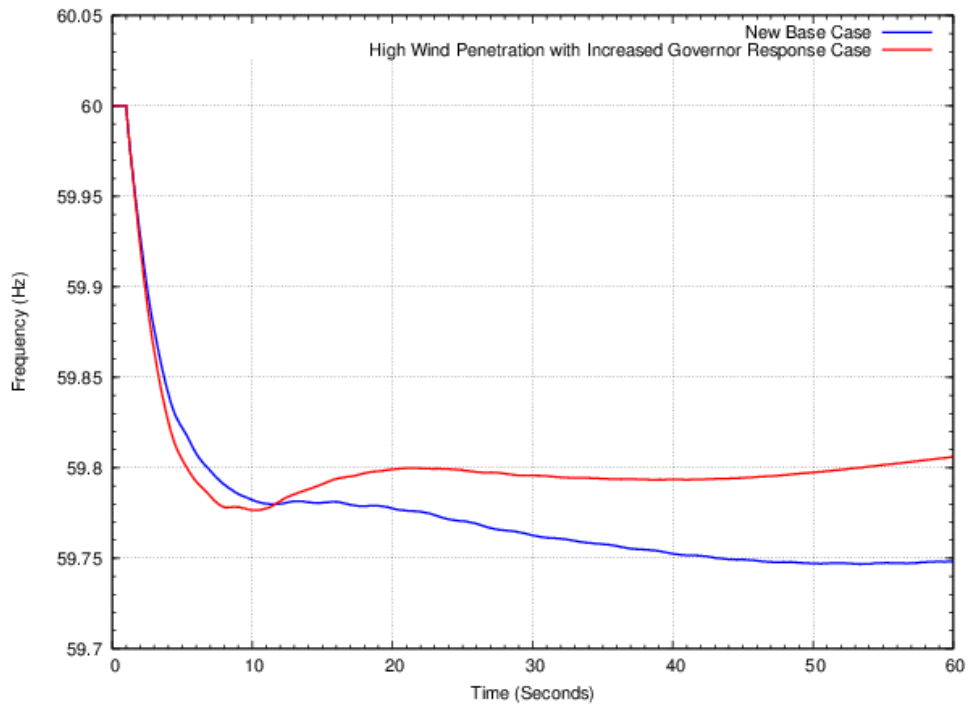

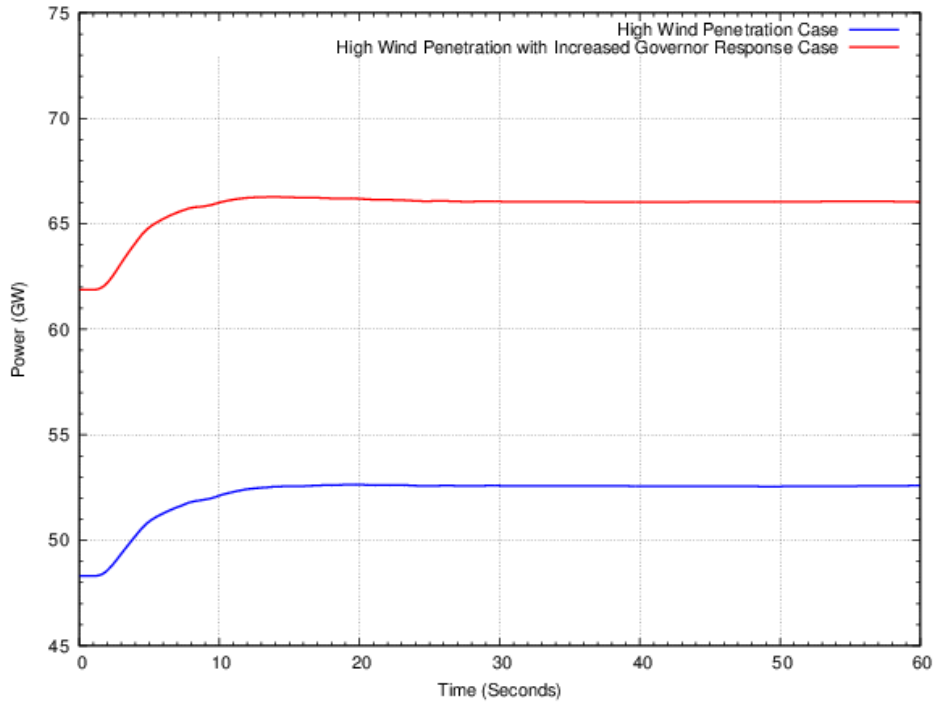**Figure 20. FR comparison – new base versus increased GR cases**

33

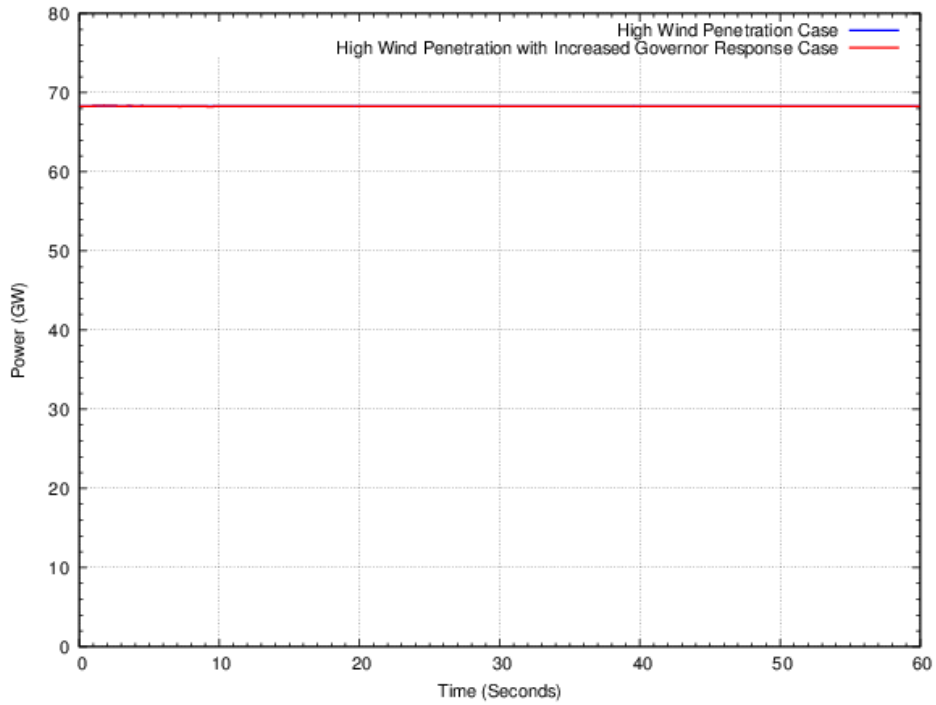**Figure 21. GR comparison – high wind penetration versus increased GR cases**

Figure 22. WTG power – high wind penetration and increased GR cases
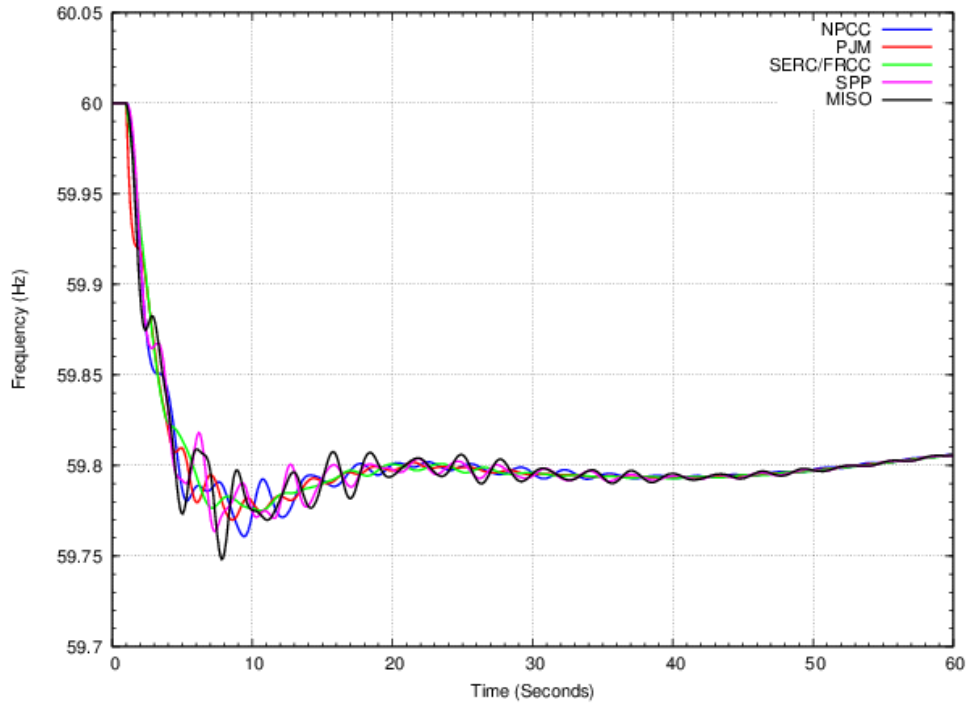
34

Figure 23. Study area FR – high wind penetration with increased GR case

Table 13 gives the frequency performance metrics for this increased GR case. The Kt of this case and the new base case (Table 8) are nearly identical, and as seen in Figure 20, the frequency nadirs are similar in both cases. The FR of this case (2,053 MW/0.1 Hz) is improved over that of the new base case (1,728 MW/0.1 Hz). This improvement results primarily from fewer thermal units with governor withdrawal. This supports the overall expectation that the amount of governors participating in FR, along with the amount of generation withdrawal, is a much more important metric than the amount of wind power.

This simulation also suggests that the location of GR units is not necessarily critical to overall EI FR. In this case, SERC/FRCC disproportionally supports the system frequency with no obvious adverse consequences. More discussion of the impact of frequency-responsive generation location is provided in Section 5.4.

Table 13. Study Area FR – High Wind Penetration Case with Increased GR

	FR (MW/0.1 Hz)	% of EI FR	FRO (MW/0.1 Hz)	Margin FR-FRO
EI	2,053	100	1,002	1,051
NPCC	386	18.8	155	231
PJM	123	6	295	−172
SERC/FRCC	1,367	66.6	399	968
SPP	84	4.1	61	23
MISO	92	4.5	93	−1

35

5.2 Governor Response from Wind Plants

When the system is under a high stress condition that results in a shortage of GR units and headroom, wind generation can contribute to primary FR. This can be achieved by curtailing wind plant power to less than that available in the wind. The potential for wind generation to respond quickly makes this resource effective in arresting and correcting frequency deviations, similar to a fast GR from thermal generation.

In this case, a fraction (about 5%) of the wind generation is curtailed with a governor-like response enabled. Specifically, approximately 90% of all the WTGs are equipped with standard 5% droop, 36-mHz deadband governors. This condition adds a total of 3.4 GW of headroom, which is about 5% of the total wind generation at this instant. The dynamic response of the wind governors is based on the GE frequency droop control feature as modeled in an internal GE version of PSLF. These governors did not have a runback or withdrawal function. The models are available in the most recent public release of PSLF.

The system response to the loss of 4,455 MW of generation for this case is shown by the red trace in Figure 24. The FR, in terms of both frequency nadir and settling frequency, was improved in comparison to the high wind case. The frequency nadir, 59.77 Hz, occurs 6.62 s after the event. For comparison, the system response to the same loss of 4,455 MW of generation for the high wind penetration case is shown by the blue trace in Figure 24. The addition of 3.4 GW of GR from the wind plants improves the frequency nadir by about 45 mHz and the settling frequency by about 140 mHz. By comparison, a similar improvement in the frequency nadir, 50 mHz, was achieved by adding 13.6 GW of GR synchronous machines.

Figure 25 shows the comparison of total synchronous machine GR and Figure 26 shows the comparison of wind power generation. The relative performance of the wind plants and the synchronous GR units is of interest. With contributions from the wind plants, the need for the synchronous machines to contribute is reduced—they settle at a lower incremental output than the case without the wind plants participating. There is also some overshoot by the synchronous governors, which are collectively faster than the wind plants *as modeled*. This raises interesting questions of system control and response because it is possible for the wind plant speed of response to be increased. The next section sheds some further light on these questions. The FR of the study areas is shown in Figure 27.

This case shows that primary FR from wind generation has the potential to greatly improve overall EI frequency performance It further suggests that the efficacy of this control, in terms of benefit per megawatt of reserve, can be substantially greater than that of thermal generation.
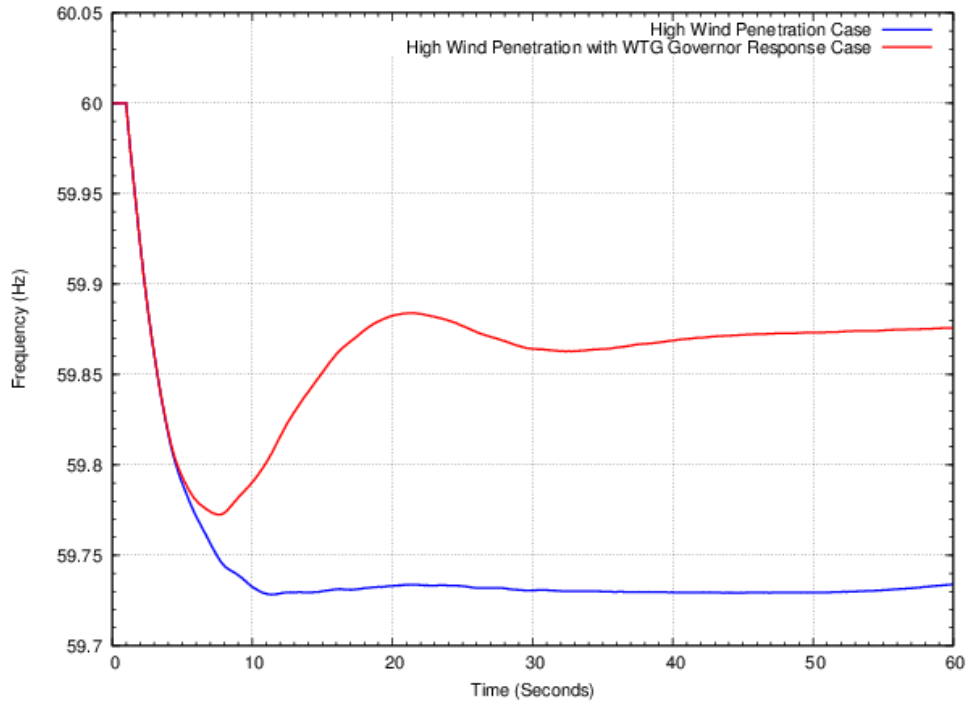
36

**Figure 24. FR comparison – high wind penetration
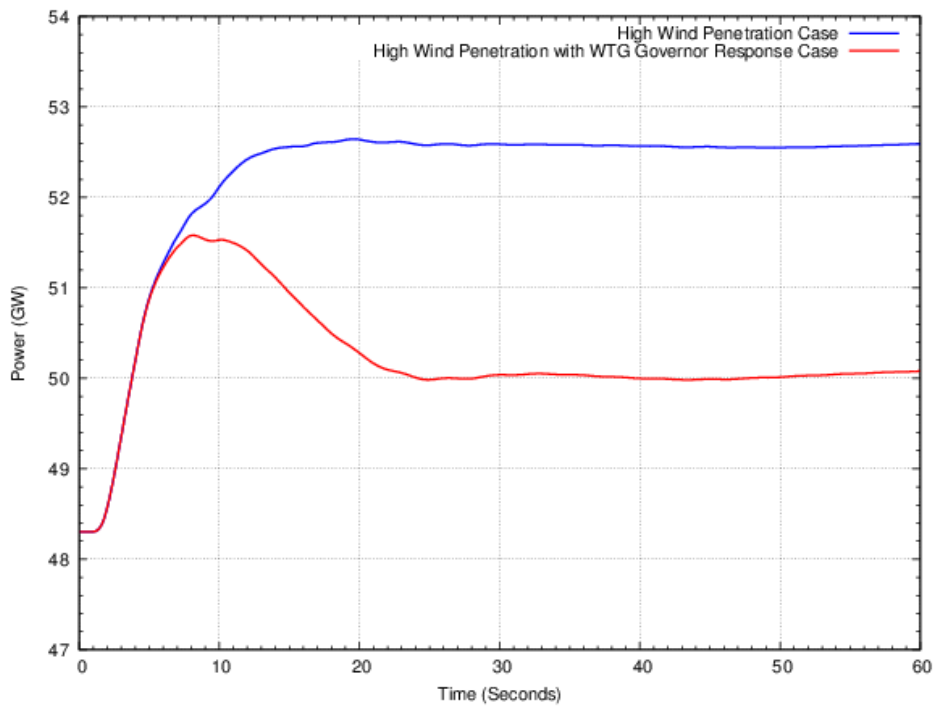versus high wind penetration with WTG GR cases**

**Figure 25. GR comparison – high wind penetration
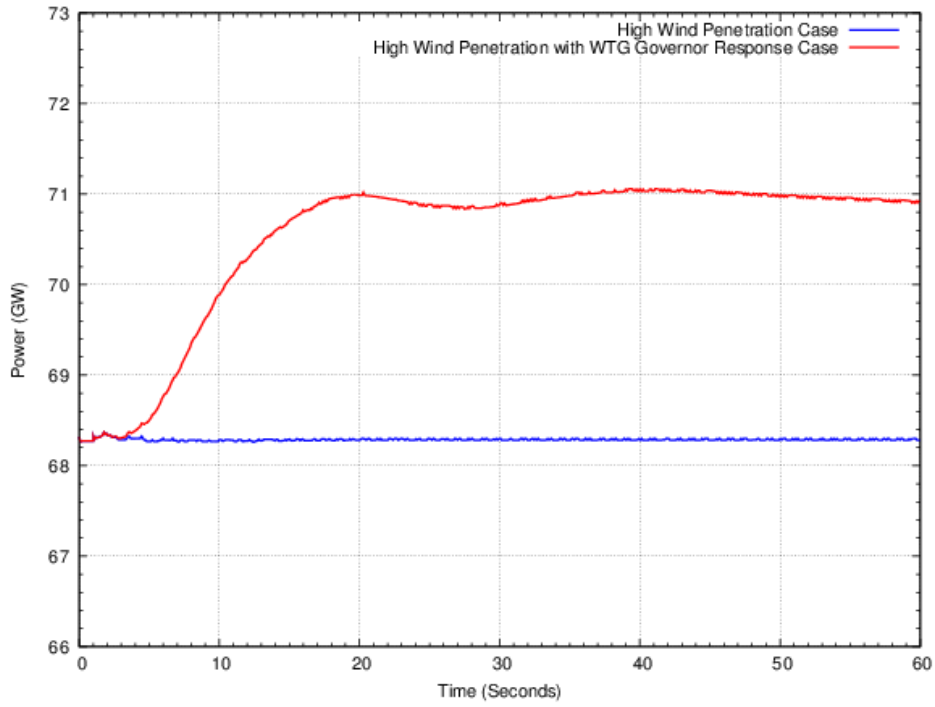versus high wind penetration with WTG GR cases**

Figure 26. WTG power comparison – high wind penetration versus high wind penetration with WTG GR cases
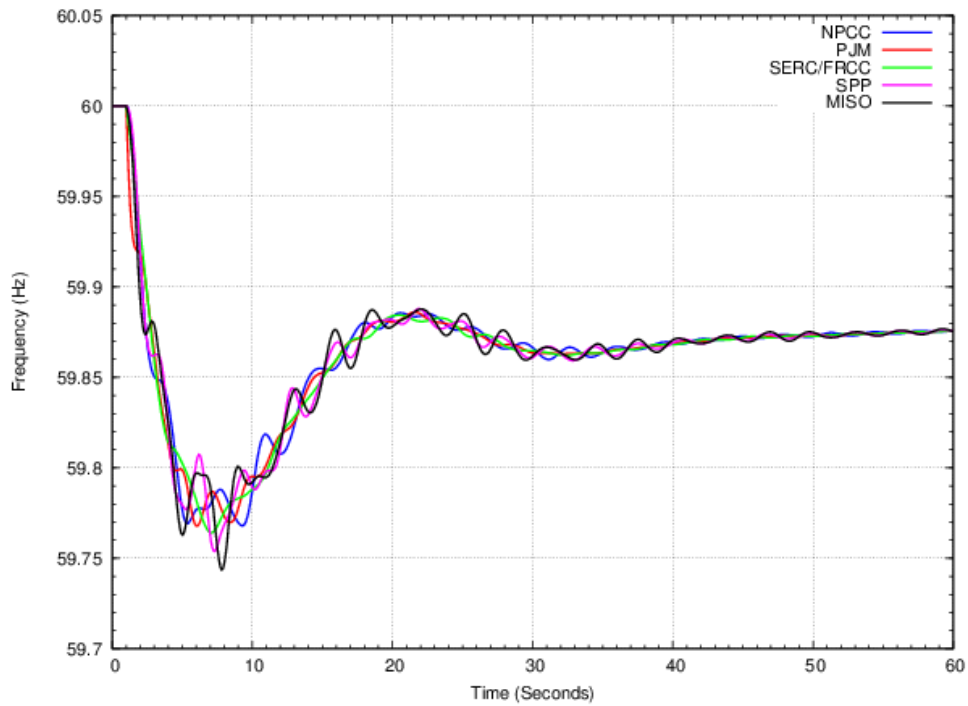

Figure 27. Study area FR with WTG GR

38

Table 14 gives the frequency performance metrics for this case with governor-responsive wind plants. The wind contribution is substantial. It more than doubles the EI frequency response, furnishing about 60% of the total. Note that the FR from GR conventional plants in the column headed "GR" dropped from 1,728 MW/0.1 Hz in the new base case to 1,325 MW/0.1 Hz with GR wind plants. This is consistent with Figure 25, and expected. The FR is spread among more machines, both conventional and wind, in this case.

Table 14. Study Area FR – High Wind Penetration with Wind GR

	FR (MW/0.1 Hz)			% of EI FR	FRO (MW/0.1 Hz)	Margin FR-FRO
	GR	Wind	Total			
EI	1,325	2,033	3,358	100	1,002	2,356
NPCC	417	526	942	28.1	155	787
PJM	78	1,042	1,120	33.4	295	825
SERC/FRCC	668	0	668	19.9	399	269
SPP	76	181	257	7.6	61	196
MISO	86	285	371	11.1	93	279

5.3 Governor Response and Inertial Controls from Wind Plants

The previous case shows that speed of response is important. In this case, all of the wind turbines that had GR in the previous case now have inertial controls as well. These inertial controls provide a means to increase the FR in the critical period before the frequency nadir. This case is based on the current GE offering (Miller et al. 2009) as represented in the PSLF model. Comparisons of the three high wind cases are shown in Figure 28, Figure 29, and Figure 30. For all three figures, the blue trace shows the response of the original high wind penetration case, the red trace shows the response of the GR from wind case, and the green trace shows the response of the GR and inertial controls from wind case.

As shown in Figure 28, FR, especially the frequency nadir, is better with both governor and inertial controls on wind plants than with governor controls alone. The inertial control arrests the frequency drop and postpones the time of the frequency nadir. The power output from GR synchronous units is shown in Figure 29. Figure 30 shows the power output of the wind plants. The difference between the green and red traces is the contribution of the inertial control, which rapidly increases the output by about 2 GW. An important consideration with inertial control by wind turbines is that the additional output is drawn from the stored inertial energy of the rotor. This energy must be returned to the machine. Until it is returned, the wind machines are running at a suboptimal speed and reduced power output. This payback period can be seen in Figure 30, when the power output of the inertial control case (green trace) drops below that of the governor-only case (red trace). In this case, the depth of the frequency nadir is improved by a further 33 mHz compared to only GR from the wind plants.

A degree of overshoot is evident in both the red and green traces of GR from the synchronous machines, as shown in Figure 29. This behavior is acceptable, but suggests

the need for prudent design of systems with high control gains. Because wind plants have the same or greater flexibility as these synchronous machines in the setting of transient governor gains, system planners should take care to avoid instabilities while maximizing the system benefit from these highly responsive controls.

Figure 31 shows the FR for the study areas. Adding inertial controls on the wind plants has some impact on the area frequencies during the first few seconds of the event. Note that the frequency of the SERC/FRCC area is substantially improved even though there are no wind plants in this region. This behavior complements the behavior shown in Figure 23, where adding FR governors in SERC/FRCC substantially improved the frequency of all the other areas. The damping is slightly better than in the case with only the governor controls, and continues to be noticeably better than in the new base case.

Figure 32 shows a comparison of the EI FR with high wind and both governor and inertial controls added to the new base case. System frequency performance is significantly better with high wind penetration and both types of FR controls. The high speed of response from the wind turbine governors, aided by the even faster inertial response, is responsible for this substantially improved performance. This improvement is a function of speed of response, and is not specific to wind power—fast governors on other types of units would have similar benefits. In short, speed of response is an important contributor to improving the frequency nadir.
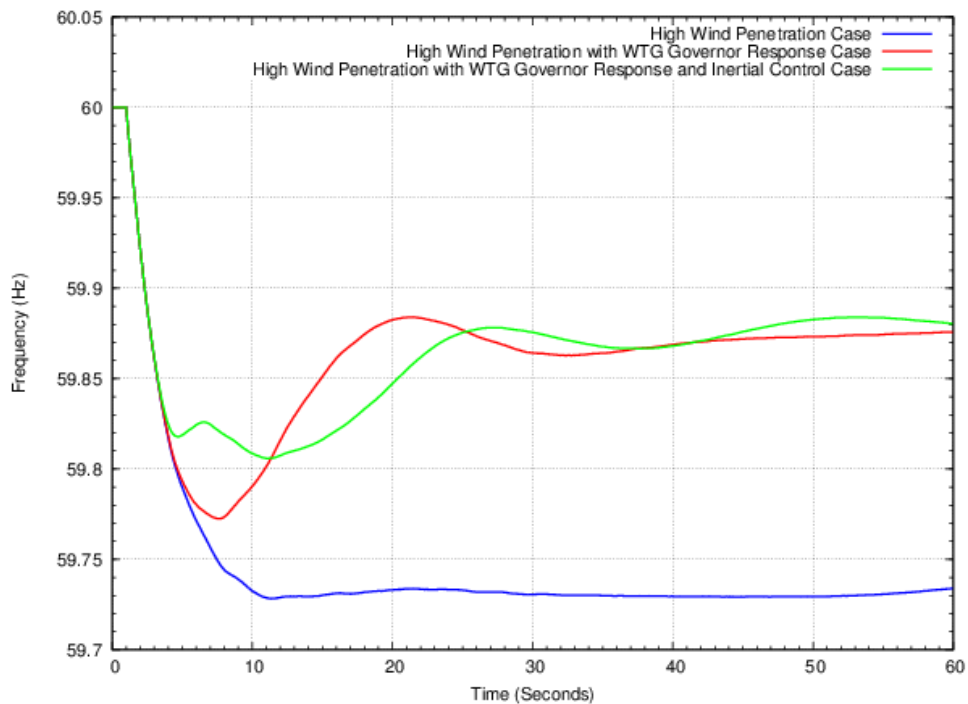

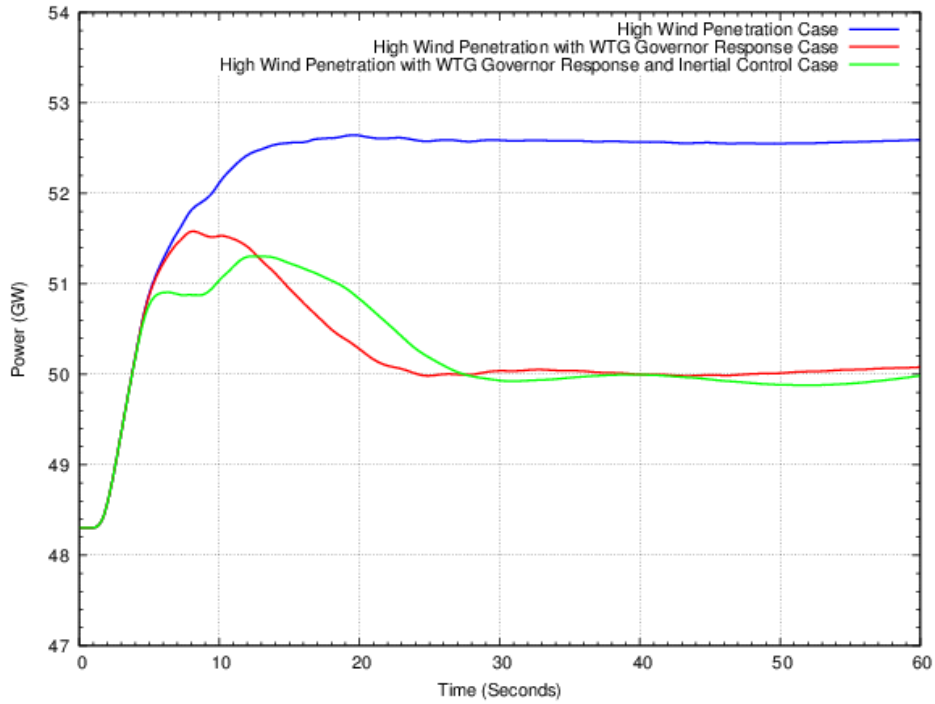**Figure 28. FR comparisons – high wind cases**

Figure 29. Synchronous GR comparison – high wind cases
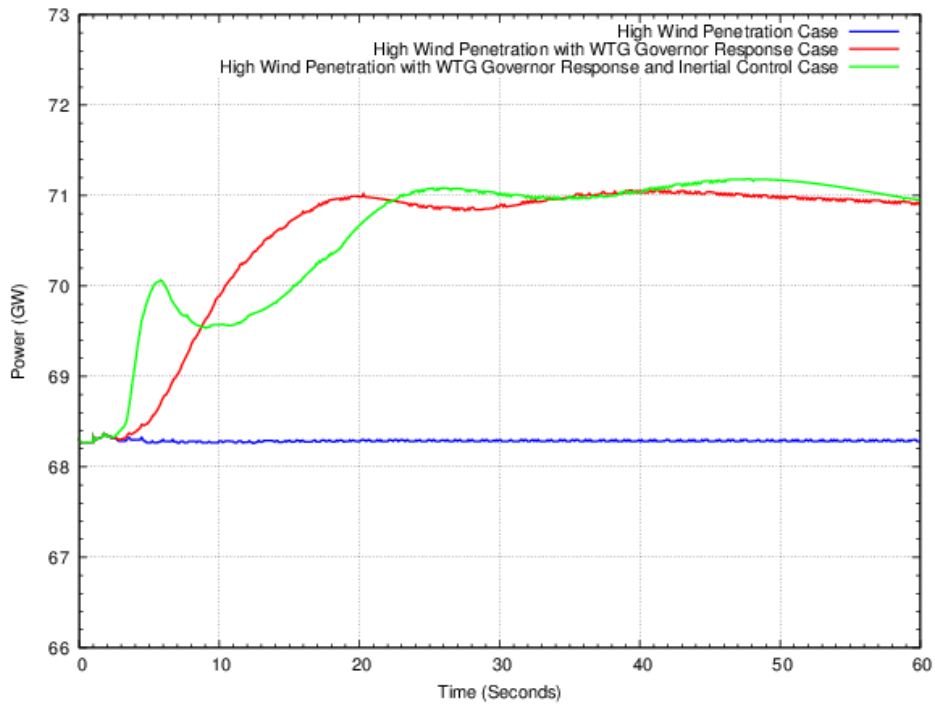
Figure 30. WTG power comparison – high wind cases

41
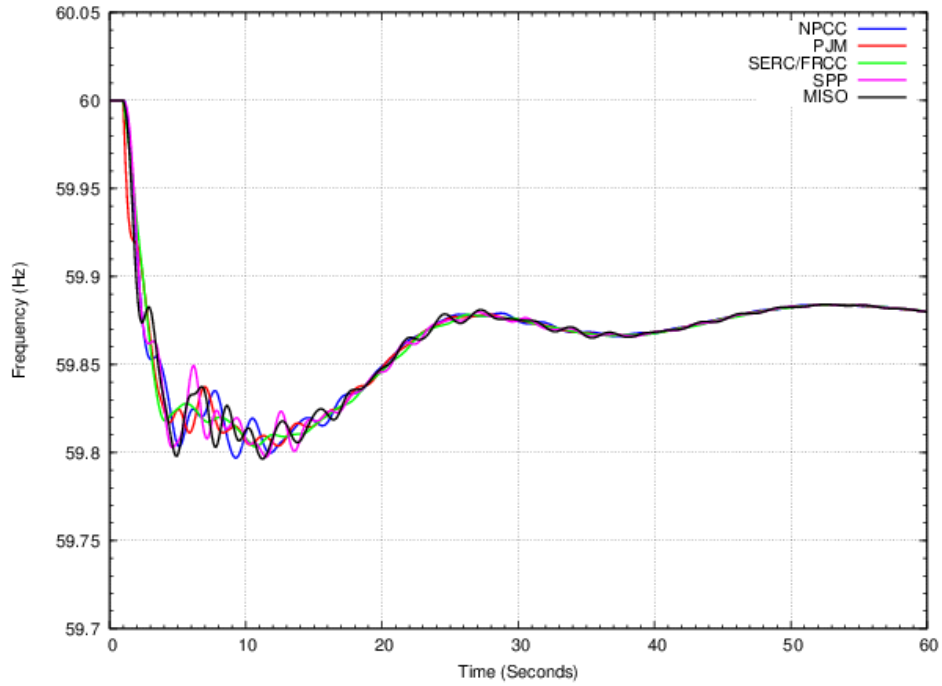
Figure 31. Study area FR – high wind with governor and inertial response case
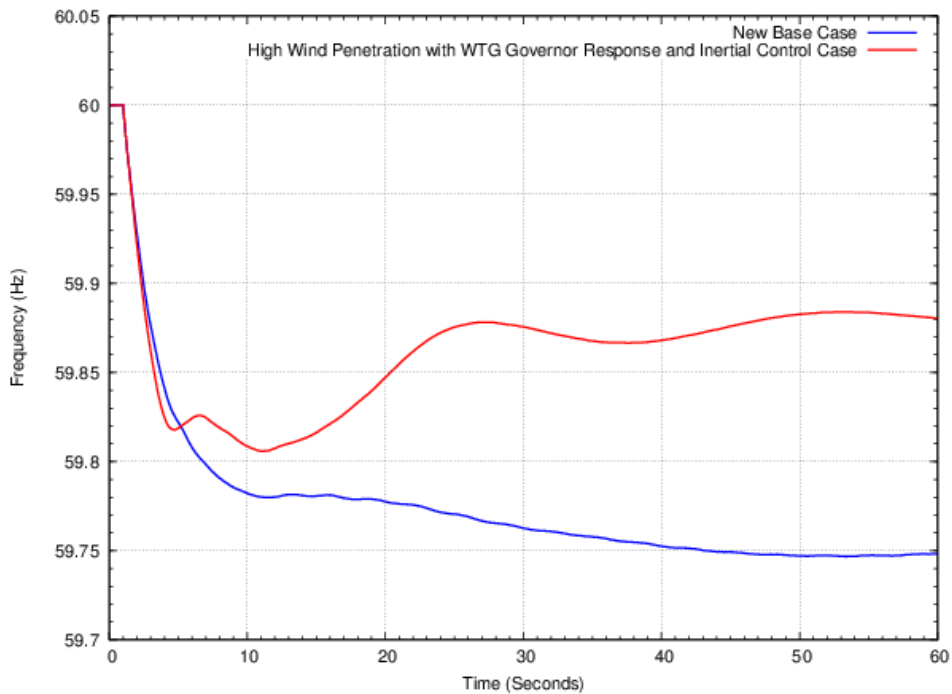
**Figure 32. FR comparison – new base case
versus high wind with governor and inertial response**

Table 15 gives the frequency performance metrics for this case with both governor and inertial response from wind plants. The FR metric is improved by inertial response from 1,758 MW/0.1 Hz in the new base case to 3,508 MW/0.1 Hz. The substantially improved frequency nadir and the change in the relative value of the frequency nadir and the settling

frequency, as shown in Figure 32, is a significant change from the current reality of the EI FR. This performance could substantially affect the NERC FRO. Specifically, the CB_R metric would increase from 1.0 to about 1.7 in this case—a value more in line with that observed in WECC and the Electric Reliability Council of Texas. This would result in an increase in the magnitude of FRO on the order of 600 to 700 MW/0.1 Hz. In other words, measures that result in a settling frequency higher than the frequency nadir will tend to increase the FRO. As a result, FR wind generation could help the system operate more securely and meet its FRO, but might also increase the mandated level of FRO.

Table 15. Study Area FR – High Wind Penetration Case
With WTG Governor and Inertial Response

	FR (MW/0.1 Hz)			% of EI FR	FRO (MW/0.1 Hz)	Margin FR-FRO
	GR	Wind	Total			
EI	1,352	2,156	3,508	100	1,002	2,506
NPCC	432	560	992	28.3	155	837
PJM	82	1,106	1,189	33.9	295	894
SERC/FRCC	671	0	670	19.1	399	272
SPP	78	191	269	7.7	61	208
MISO	89	301	389	11.1	93	297

5.4 Location of Governor-Responsive Generation

A comparison of system frequency response between Case 5 (high wind with increased governor response from conventional units) and Case 6 (high wind with governor response from wind plants) or Case 7 (high wind with governor and inertial response from wind plants) must be done with care. As noted in Section 5.1, all of the incremental governor response of Case 5 was provided by enabling control in the SERC/FRCC study area. This area is not host to the added wind generation and is relatively remote from the site of the disturbance in Indiana. The common-mode frequency, as shown in Figure 19, is the primary measure of system performance, but this is an analytical construct. Individual synchronous generators respond to changes in their own speed, which has a substantial locational aspect. The green trace in Figure 23 is representative of the frequency in the southeast. The governors in that area respond to unit speeds that more closely resemble that trace. In cases 6 and 7, the wind plants are subject to frequencies that resemble the traces in their respective areas. This means that a megawatt-to-megawatt comparison between synchronous machine governor response in the southeast and wind plant governor response distributed across the wind plants in the rest of the EI is imperfect. If a similar size (i.e., ~4,500-MW) event occurred at a different location in the EI, the common-mode frequency would probably not change dramatically, but the individual unit speeds and frequencies would be different, and therefore the unit responses would be different. As noted in the discussion of Case 5, there is no indication that having extra frequency response provided remote from the event (i.e., in the southeast for an event in Indiana) creates problems. However, inter-area transmission limitations might adversely impact the deliverability of the extra power from frequency-responsive generation. This is an area that would benefit from further investigation.

6 Summary, Conclusions and Recommendations

6.1 Summary and Conclusions

Figure 33 illustrates the evolution of the study cases. Cases 1 and 2 were steps in the development of a new base case (case 3) that more realistically represents EI FR with a low level of wind penetration. Cases 4 through 7 had a high penetration of wind generation with variations in both thermal and wind generation FR.
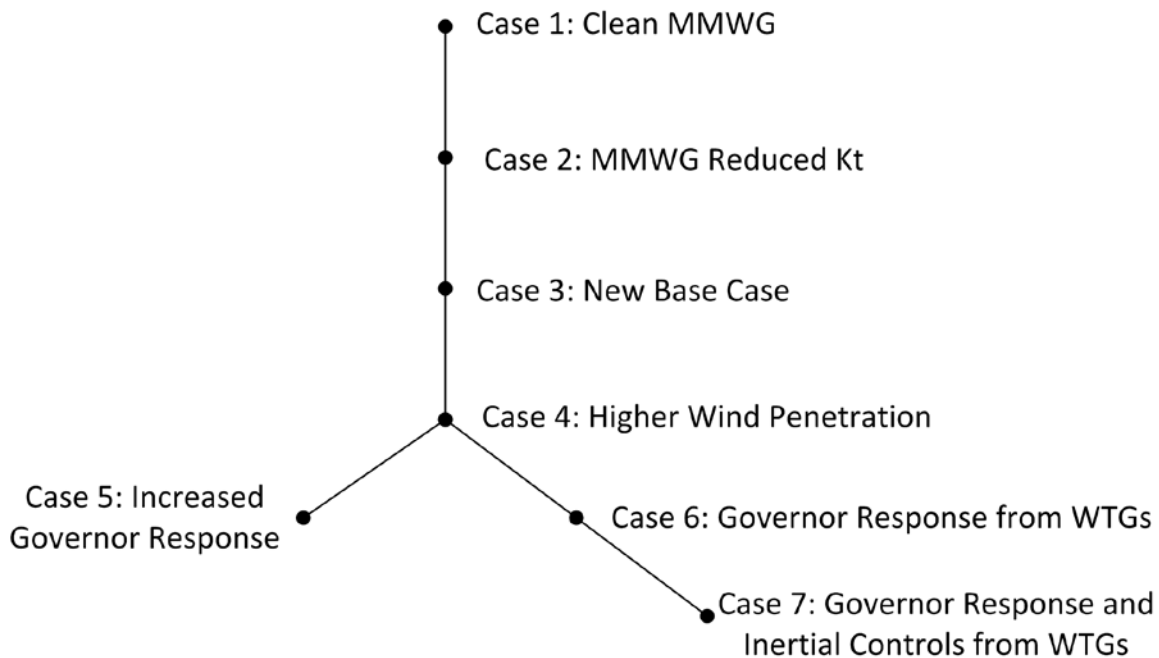
Case 1: Clean MMWG

Case 2: MMWG Reduced Kt

Case 3: New Base Case

Case 4: Higher Wind Penetration

Case 5: Increased Governor Response

Case 6: Governor Response from WTGs

Case 7: Governor Response and Inertial Controls from WTGs

Figure 33. Evolution of study cases

Figure 34 shows a comparison of the EI FR for all cases. Table 16 gives an overall summary of the EI frequency performance for each case when subject to the same 4,455-MW generation outage. This table lists the primary factors that affect FR (i.e., the percentage of generation providing GR, Kt, and withdrawal), and the metrics used to measure frequency performance. Note that headroom is not shown because it was not an issue for any of the simulations.

These results show the strong correlation between the amount of GR generation (Kt), the withdrawal behavior of the responsive generation after an event, the speed of control response, and the overall frequency performance of the grid. This is consistent with findings of NERC, LBNL, and others (NERC 2012c, Eto, J. et al. 2010).

The analysis shows that the responsiveness of generation dictates FR, not the type of generation that provides the response. Increased Kt, reduced withdrawal, and faster response will improve system FR. Whether this response is from conventional thermal generation or from wind generation makes little difference. Location of responsive generation was not examined in detail for this study but warrants careful consideration. There is no evidence that adding wind generation will inevitably degrade FR. In addition, technical options currently exist to maintain adequate FR.
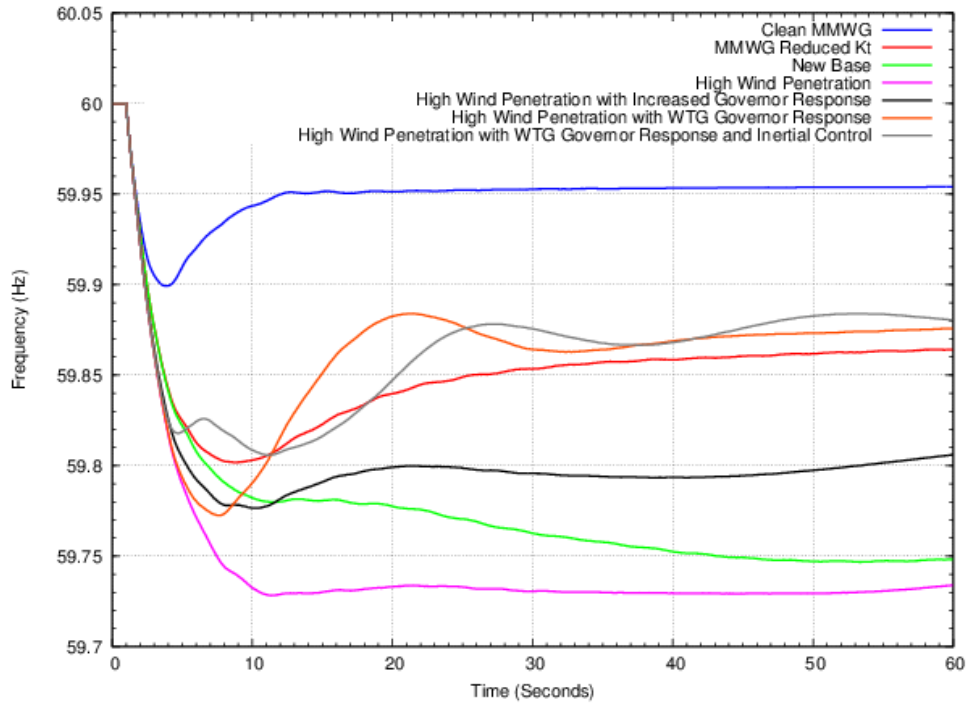
44

Figure 34. FR – all study cases

Table 16. Summary of EI Frequency Performance in Response to 4,455-MW Generation Loss for Each Study Case

Case	Kt (%)	Withdrawal	EI FR (MW/0.1 Hz)	Frequency Nadir (Hz)	Nadir Time (s)	Settling Frequency (Hz)	Comments
Target			1,002	59.5			Minimum target levels
Clean MMWG	78.9	No	9,375	59.90	2.89	59.95	Not representative of expected behavior; frequency response better than observed
MMWG Reduced Kt	32.4	No	3,058	59.80	7.87	59.86	Does not show Lazy-L effect
New Base Case	32.4	Yes	1,728	59.75	52.5	59.75	Reasonable match to expected
High Wind Penetration	26.8	Yes	1,583	59.73	10.36	59.73	High wind penetration, no deliberate maintenance of thermal response; degraded frequency performance
High Wind Penetration with Increased GR	32.3	Yes but reduced from 4	2,053	59.78	9.21	59.81	Increased Kt and reduced withdrawal from thermal units improves frequency performance
High Wind Penetration with WTG GR	26.8[a]	Yes[b]	3,358	59.77	6.62	59.88	WTG GR (increased Kt, no withdrawal) improves frequency performance
High Wind Penetration with WTG GR and Inertial Control	26.8[a]	Yes[b]	3,508	59.80	10.08	59.88	WTG GR (increased Kt, no withdrawal) plus inertial response gives best performance of realistic cases

[a] Kt values for cases 6 and 7 do not include the effect of regulation from wind turbines.
[b] Wind turbines do not have withdrawal.

6.2 Recommendations

The standard MMWG dynamic data set exhibits FR that bears little resemblance to the observed behavior of the EI, which was recognized before this study. The wholesale generic modifications to the data set used in this study were necessary to match observed FR and could be considered a substantial improvement.

Recognizing that it represents a massive undertaking, a system-wide and plant-specific improvement to the modeling of the EI is recommended. Efforts are already under way in various regions to improve overall dynamic modeling, including that of governors. Those should continue, and arguably should be broadened and accelerated. In the interim, the EI (through the MMWG or other mechanisms) should consider implementing more generic rules on governor modeling based on plant type and known controls.

This investigation was of limited scope. Additional study of the EI, including a wide range of possible operating conditions, along with various commitment and dispatch strategies with high levels of wind power, is recommended. Other aspects, including the impact of governor headroom and deadband, load modeling, location of responsive reserves, and response to overfrequency events, should also be examined.

Load controls without frequency bias are known to cause governor withdrawal. This study reinforces other work that identified this behavior as a significant concern. Further investigation into the institutional causes and mitigation of this behavior is needed.

This investigation is a step toward a better understanding of the frequency behavior of the EI, and the possible impact that large amounts of wind generation might have on FR. This study does not examine the operational practice or institutional mechanisms necessary to take advantage of the technical options identified, nor does it consider whether existing practice is sufficient to ensure adequate FR. This institutional investigation should proceed in parallel with the development of additional technical understanding.

7 References

Alberta Electric System Operator. (2010). *Proposed New Level 1 ISO Rules, Part 500, Facilities, Division 502, Technical Requirements, Section 502.1, Wind Aggregated Generating Facilities, Technical Requirements, External Draft 2.0.* May 6. Calgary: Alberta Electric System Operator.

EirGrid (2011). *EirGrid Grid Code, Version 3.5.* Effective March 15. Dublin: EirGrid. Accessed February 23, 2013:
http://www.eirgrid.com/media/2011%20Mar%2008%20EirGrid%20Grid%20Code%20Clean%20Version%203.5.pdf.

Electric Reliability Council of Texas (2010). "Primary Frequency Response Requirement From Existing WGRs." PRR833. Approved on May 18.

Eto, J. et al. (2010). *Use of Frequency Response Metrics to Assess the Planning and Operating Requirements for Reliable Integration of Variable Renewable Generation.* LBNL-4142E. Berkeley, CA: Lawrence Berkeley National Laboratory.

GE Energy (May 2010). *Western Wind and Solar Integration Study.* NREL/SR-550-47434. Golden, CO: National Renewable Energy Laboratory. Accessed February 22, 2013: http://www.nrel.gov/docs/fy10osti/47434.pdf.

Miller, N.W.; Clark, K.; Shao, M. (2011). "Frequency Responsive Wind Plant Controls: Impacts on Grid Performance." *Power and Energy Society General Meeting, 2011 IEEE.* Piscataway, NJ: IEEE.

Miller, N.W.; Shao, M.; Venkataraman, S. (2011). *California ISO (CAISO) Frequency Response Study, Final Draft.* Schenectady, NY: GE Energy. Accessed February 22, 2013: http://www.caiso.com/Documents/Report-FrequencyResponseStudy.pdf.

Miller, N.; Clark, K.; Walling, R. (2009). "WindINERTIA: Controlled Inertial Response from GE Wind Turbine Generators." Presented at the 45th Annual Minnesota Power Systems Conference, Minneapolis, Minnesota, November.

NERC (2012a). *Standard BAL-003- Frequency Response and Frequency Bias Setting.* November 30.

NERC (2012b). *Standard BAL-003-1, Attachment A - Frequency Response and Frequency Bias Setting –Supporting Document.* November 30. http://www.nerc.com/docs/standards/sar/Attach_A-Frequency_Response_Standard_Support_Document-Clean.pdf

NERC (2012c). *Frequency Response Initiative Report.* Draft. September 30. http://www.nerc.com/docs/pc/FRI%20Report%209-30-12%20Clean.pdf

NERC (2012d). *Standard BAL-003-1, Attachment A.* Draft. February 12.

NERC (2009). *Standard Models for Variable Generation.* Special Report. Princeton, NJ: NERC. Accessed February 23, 2013: http://www.nerc.com/docs/pc/ivgtf/IVGTF_Report_PhaseII_Task1-1_Final(5.24).pdf.

NERC (2004). "Frequency Response Standard Whitepaper." April 6. Princeton, NJ: NERC. Accessed February 23, 2013: http://www.nerc.com/docs/oc/rs/Frequency_Response_White_Paper.pdf.

Sanchez-Gasca, J.J.; Miller, N.W.; Price, W.W. (2004). "A Modal Analysis of a Two-Area System with Significant Wind Power Penetration." *Power Systems Conference and Exposition, 2004. IEEE PES.* Schenectady, NY: IEEE.

Undrill, J. (2010). *Power and Frequency Control as it Relates to Wind-Powered Generation.* LBNL-4143E. Berkeley, CA: Lawrence Berkeley National Laboratory.

WECC (2012). *Composite Load Model for Dynamic Simulations.* Report 1.0. WECC Modeling and Validation Work Group. Accessed February 23, 2013: http://www.wecc.biz/committees/StandingCommittees/PCC/10102012/Approval%20Items/1/WECC%20MVWG%20Load%20Model%20Report%20ver%201%200.pdf